FOR OFFICIAL USE ONLY

JPRS L/8527

20 June 1979

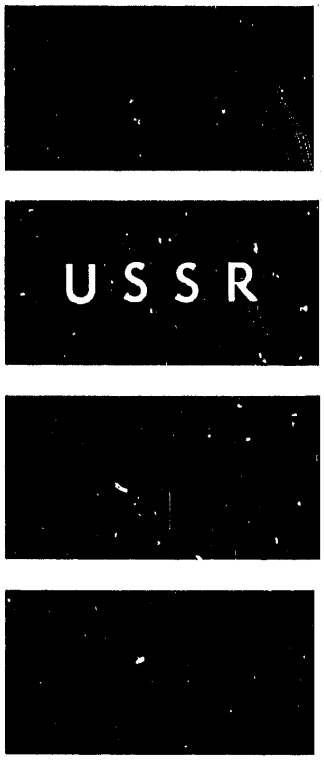

TRANSLATIONS ON USSR SCIENCE AND TECHNOLOGY
PHYSICAL SCIENCES AND TECHNOLOGY
(FOUO 33/79)
QUANTUM ELECTRONICS

U. S. JOINT PUBLICATIONS RESEARCH SERVICE

FOR OFFICIAL USE ONLY

NOTE

JPRS publications contain information primarily from foreign newspapers, periodicals and books, but also from news agency transmissions and broadcasts. Materials from foreign-language sources are translated; those from English-language sources are transcribed or reprinted, with the original phrasing and other characteristics retained.

Headlines, editorial reports, and material enclosed in brackets [] are supplied by JPRS. Processing indicators such as [Text] or [Excerpt] in the first line of each item, or following the last line of a brief, indicate how the original information was processed. Where no processing indicator is given, the information was summarized or extracted.

Unfamiliar names rendered phonetically or transliterated are enclosed in parentheses. Words or names preceded by a question mark and enclosed in parentheses were not clear in the original but have been supplied as appropriate in context. Other unattributed parenthetical notes within the body of an item originate with the source. Times within items are as given by source.

The contents of this publication in no way represent the policies, views or attitudes of the U.S. Government.

APPROVED FOR RELEASE: 2007/02/09: CIA-RDP82-00850R000100060038-3

JPRS L/8527

20 June 1979

TRANSLATIONS ON USSR SCIENCE AND TECHNOLOGY
PHYSICAL SCIENCES AND TECHNOLOGY

(FOUO 33/79)

QUANTUM ELECTRONICS

Moscow KVANTOVAYA ELEKTRONIKA in Russian Vol 6 No. 3, 1979
pp 466-472, 513-517, 548-552, 592-593, 597-598, 629-631, 635-641
646-648

CONTENTS PAGE

CONTENTS (Continued) Page

QUANTUM ELECTRONICS

UDC 535.21

THE INFLUENCE OF INTERFERENCE EFFECTS IN OXIDE FILMS ON THE DYNAMICS OF METAL HEATING USING LASER RADIATION

Moscow KVANTOVAYA ELEKTRONIKA in Russian Vol 6 No 3, 1979 pp 466-472

[Article by M.I. Arzuov, A.I. Barchukov, F.V. Bunkin, N.A. Kirichenko, V.I. Konov and B.S. Luk'yanchuk, Physics Institute imeni P.N. Lebedev of the USSR Academy of Sciences, Moscow, manuscript received 6 Apr 78]

[Text] A theoretical model is constructed for the oxidation of metals by continuous laser radiation, taking into account interference phenomena in the oxide film. The problem is solved by the simultaneous solution of a parabolic equation for the kinetics of metal oxidation, the thermal conductivity equation taking convective and radiative losses into account, as well as an equation which relates the absorptivity of the oxide--metal system to the thickness and the optical constants of the oxide film, as well as the cold absorptivity of the metal. Heating kinetics are analyzed from room temperature up to the melting point of the thermally thin plate and the semi-infinite target. The results of the calculations are in good agreement with the experimental data for the oxidation of copper by the radiation of a CW CO_2 laser.

1. Introduction

As was noted in the literature [1-7], the interaction of CO_2 laser radiation with metals in an oxidizing atmosphere possesses a number of special features. When metals are irradiated in a neutral gas medium or in a vacuum, their absorptivity for radiation at the long wavelength of 10.6 μm, as a rule, proves to be small. However, when irradiated in an oxidizing atmosphere, an oxide film is formed on the surface of the metal which has a considerable molecular absorptivity [8]. With an increase in the oxide film thickness, the absorptivity changes, and correspondingly, the rate of temperature increase changes. To compute the process of metal heating in an oxidizing atmosphere, it is

necessary to simultaneously solve the equations of thermal conductivity and metal oxidation kinetics taking into account the change in metal absorptivity during oxidization. Papers [2 - 6] were devoted to an approximate solution of this problem.

The law governing the growth of the oxide film depends on its thickness. It was shown in paper [5] that the growth thin ($x < 100$ nm) oxide layer continues for a relatively brief time, and this stage of the process does not play a substantial part in the problem of metal heating with CO_2 laser radiation. If the thickness of the film is $x \geq 100$ nm, then the oxidation kinetics equation has the form

$$\frac{dx}{dt} = \frac{d}{x} e^{-T_д/T}, \tag{1}$$

where t is time; $T_д$ is the diffusion activation energy or an ion of the metal (or oxygen) in the oxide; T is the temperature, °K; the constant d is related to the diffusion factors for the metal and oxygen ions in the oxide layer [9]. The thickness of the oxide layer determines the absorptivity A of the metal. It was assumed in papers [2, 3] that:

$$A = A_0 + 2\alpha x, \tag{2}$$

where A_0 is the absorptivity of the metal in the absence of the oxide film; α is the radiation absorption factor in the oxide.

It is demonstrated in this paper that in the process of continuous heating of a metal, the thickness of the oxide film becomes comparable to the radiation wavelength, and formula (2) cannot be used. Moreover, during the growth of the oxide film, oscillations in the absorptivity can arise in it by virtue of interference phenomena in the oxide--metal layer system, which must likewise be taken into account.

2. The Absorptivity of a Layered System

The absorptivity A is expressed in terms of the values of the optical characteristics of the oxide and metal. For the case of normal incidence of the radiation, we have [10]:

$$A = 1 - |R|^2; \quad R = \frac{r_{12}\exp(-2i\psi) + r_{23}}{\exp(-2i\psi) + r_{12}r_{23}};$$
$$\text{где } \psi = \frac{\omega}{c} x \sqrt{\varepsilon} = \frac{1}{2}(\beta + i\alpha)x; \quad r_{12} = \frac{1 - \sqrt{\varepsilon}}{1 + \sqrt{\varepsilon}}; \quad r_{23} = \frac{r_{12} - r_{13}}{r_{12}r_{13} - 1}; \tag{3}$$
$$\text{where } 1 - |r_{13}|^2 = A_0;$$

ω is the radiation frequency, c is the speed of light, r_{12} and r_{13} are the radiation amplitude reflection factors from the oxide and from the metal; ε is the oxide dielectric permittivity; $\sqrt{\varepsilon} = n + i\kappa$; $\alpha = 2\kappa\omega/c$ is the oxide absorption factor; $\beta = 2n\omega/c$. For good conductors [10], $A_0 \ll 1$, and $r_{13} = -1 - 0.5A_0(i - 1)$.

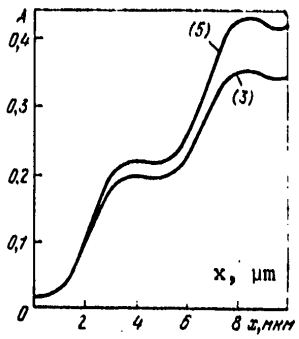

Figure 1. The function A(x) for the case of n = 1.098 and x = 0.019, plotted from formulas (3) and (5):

$A_{1max}(3) = 0.199$;
$A_{1min}(3) = 0.196$;
$A_{1max}(5) = 0.222$;
$A_{1min}(5) = 0.218$.

A graph of the function A(x) plotted from formula (3) is shown in Figure 1. As can be seen from Figure 1, the absorptivity of a layered system is characterized by the presence of oscillations due to interference phenomena in the oxide layer.

The position of the extrema of the function A(x) is determined from the condition dA/dx = 0, which can be written in the form:

$$\text{th}\,\frac{\alpha x + l}{2}\,\text{tg}\,\frac{\beta x + \varphi}{2} = \frac{\text{Im}\sqrt{1 - 1/\varepsilon}}{\text{Re}\sqrt{1 - 1/\varepsilon}};$$

$$\text{th}\,\frac{\alpha x + l}{2}\,\text{tg}\,\frac{\beta x + \varphi}{2} = -\frac{\text{Re}\sqrt{1 - 1/\varepsilon}}{\text{Im}\sqrt{1 - 1/\varepsilon}}, \qquad (4)$$

where $l = -\ln|r_{23}|$; $\phi = \arg r_{23}$; the first equation determines the maximum points and the second the minimum points.

As a rule, at the radiation frequency of a CO_2 laser, the following conditions are met: $1 - |r_{12}|^2 \gg A_0$, $\kappa \ll 1$, and $n > 1$. Then within a precision of first order terms with respect to κ and A_0, we have:

$$\frac{\text{Im}\sqrt{1 - \frac{1}{\varepsilon}}}{\text{Re}\sqrt{1 - \frac{1}{\varepsilon}}} = \frac{\kappa}{n(n^2 - 1)}; \quad l = \frac{nA_0}{2}; \quad \varphi = \pi + \frac{nA_0}{2}.$$

By virtue of the condition $\alpha < \beta$ ($\alpha/\beta = \kappa/n \ll 1$), the first oscillations are characterized by small values of the optical thickness ($\alpha x \ll 1$). Taking this into account for A(x), one can derive the following approximate expression:

$$A(x) = \frac{n^2 A_0 + 2\kappa(\beta x - \sin\beta x)}{n^2 + (1 - n^2)\sin^2(\beta x/2)}, \qquad (5)$$

where the position of the maxima is determined by the equation:

$$\text{tg}\,\frac{\beta x}{2} = (1 - n^2)\left[\frac{\beta x}{2} + \frac{n^2 A_0}{4\kappa}\right], \qquad (6)$$

while the position of the minima is determined by the equation:

$$\sin\frac{\beta x}{2}=0. \tag{7}$$

A graph of the function A(x), plotted from formula (5), is also shown in Figure 1. As was indicated in paper [11], based on the values of the absorptivity at the extrema points, one can determine the optical constants of the oxide. In those cases where $n - 1 \ll 1$, $\kappa \ll 1$, $A_0 \ll 1$ and substantial values of the oxide film thickness $\Delta x \gg 1/\beta$, the following expression can be derived from (3) following averaging with respect to the period of the oscillations:

$$A(x)=1-(1-A_0)e^{-2\alpha x},$$

which within a range of $2\alpha x \ll 1$, agrees with (2).

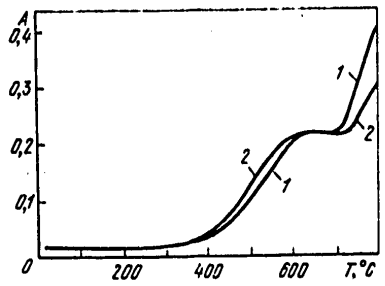

Figure 2. Theoretical (1) and experimental (2) curves of A(T) for the oxidation of copper in air:

The constants for copper and Cu_2O oxide, used in plotting the theoretical curve A(T) were taken from [10, 11]; P = 21 watts; m = 50 mg.

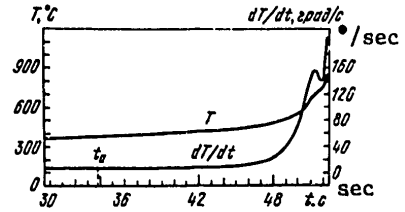

Figure 3. The theoretical functions T(t) and dT(t)/dt, taking thermal losses into account for the oxidation of copper in air at P = 21 watts, m = 50 mg and A_0 = 2%, t_a is the activation time of the oxidation reaction.

3. The Heating of a Thermally Thin Plate

In that case where the characteristic times for the change in temperature with the action of radiation are large as compared to the characteristic times for establishing the temperature through the volume of the plate, the heating of the target is described by the equation:

$$\frac{dT}{dt} = \frac{P}{mc_0} A(x), \tag{8}$$

where m is the weight; c_0 is the specific heat capacity of the metal; P is the total incident radiation power.

The function T(x) can be determined from equations (1) and (8):

$$\int_{T_н}^{T} \exp\left(-\frac{T_н}{T}\right) dT = \frac{P}{mc_0 d} \int_0^x xA(x)\,dx, \tag{9}$$

where $T_н$ is the initial temperature of the target.

By eliminating the parameter x from equations (5) and (9), we find the function A = A(T). The graph of this function is shown in Figure 2. The function A(T) which is determined in this manner allows for a description of the temperature increase dynamics by means of equations (8):

$$t = \frac{mc_0}{P} \int_{T_н}^{T} \frac{dT}{A(T)}. \tag{10}$$

In those cases where convective and radiative thermal losses having the following power play a marked part:

$$P_{loss}(T) = P_{пот}(T) = [\eta(T - T_н) + \sigma\sigma_0(T^4 - T_н^4)]s, \tag{11}$$

The quantity $A(T) - P_{пот}(T)/P$ is to be used in formula (10) in place of the quantity A(T). In formula (11), η is the convective heat exchange constant; σ is Stefan-Boltzmann's constant; σ_0 is the grayness coefficient; s is the total surface area of the target.

Graphs of the function T(t) and dT/dt, taking thermal losses into account, are shown in Figure 3.

4. The Activation Time of the Oxidation Reaction

As was noted in the literature [2, 3, 6, 7], when a metal is heated in an oxidizing atmosphere, there is a certain characteristic activation time for the oxidation reaction t_a, beginning at which the oxidation process accelerates. This point in time is conveniently determined from the position of the minimum on the y(t) = dT/dt curve, which is recorded directly during an experiment.

The cause of the existence of a minima of the function y(t) is the competition of two factors: heat exchange with the ambient medium and an increase the absorptivity due to the growth of the oxide film.

Taking heat exchange with the external medium into account, the heating of a thermallythin plate is described by the equation:

$$\frac{dT}{dt}=\frac{P}{mc_0}(A-Q), \quad Q(T)=\frac{P_{\text{пот}}(T)}{P}. \tag{12}$$

[$P_{\text{пот}} = P_{\text{loss}}$].

Since at the point in time $t = t_a$ the thickness of the oxide filmis small, then for A(x), one can make use of the expression (see (5)):

$$A(x)=A_0+bx^2, \quad b=(n^2-1)4\pi^2A_0/\lambda^2, \tag{13}$$

where λ is the radiation wavelength.

The activation time is determined from the condition $d^2T/dt^2|_{t=t_a} = 0$. In those cases where the primary contribution to thermal losses is made by convective heat exchange (in this case, the condition $T << T_д$ is clearly met), the following approximate expression can be derived for the activation time:

$$t_a=\frac{mc_0}{PA_0}\left[\frac{T_д}{L}-T_н\right], \quad L=\ln\left(\frac{2bdmc_0}{A_0\eta s}\right). \tag{14}$$

At this point in time, the temperature of the target T_a and the thickness of the oxide film x_a are correspondingly equal to:

$$T_a=\frac{T_д}{L}, \quad x_a=\frac{\eta sT_д}{Pb}\frac{1}{L^3}. \tag{15}$$

The range of applicability of formulas (14) and (15) is limited by the not excessively small values of A_0. At small values of A_0, the fact that the heating conditions are close to steady state plays a substantial part. In this case, the following quasistationary approximation can be employed to obtain the quantity t_a:

$$A=Q(T), \quad x^2=2dt\exp(-T_д/T). \tag{16}$$

Equations (13) and (16) define the function T(t) in the approximation considered here. The point of inflection on this curve defines the activation time:

$$t_a=\frac{T_c^3}{4dbT_д}\frac{\exp(T_д/T_c)}{1+T_д/2T_c}\left(2\frac{T_д}{T_c^2}\frac{dQ}{dT}-\frac{d^2Q}{dT^2}\right), \tag{17}$$

where T_c is determined by the equation $A_0 = Q(T_c)$. In particular, if only the convective thermal losses are important, formula (17) is simplified:

$$t_a = \frac{T_c \eta s}{2dbP} \cdot \frac{\exp(T_д/T_c)}{1 + T_д/2T_c}, \quad T_c = T_н + \frac{PA_0}{\eta s}. \tag{18}$$

A graph of the function $t_a(A_0)$, plotted from formulas (14) and (17), is shown in Figure 4 along with the experimental points.

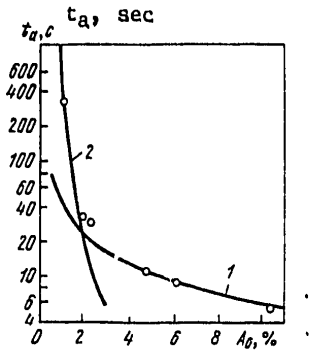

Figure 4. The activation time as a function of the "cold" absorptivity of copper.

Curve 1 was plotted from formula (14) for $d = 1.88 \cdot 10^{-3}$ cm^2/sec, and Curve 2 from formula (17) for $d = 1.59 \cdot 10^{-3}$ cm^2/sec, $\sigma_0 = 0.415$, $\eta = 2.22 \cdot 10^{-3}$ w/cm^2 · deg, $T_д = 10^4$ °K, P = 30 w, m = 85 mg, and s = 0.4 cm^2.

5. The Heating of Massive Samples

An approximation of a semi-infinite material can be employed to describe the heating of massive samples. In this case, when heating with a circular cource of radius r, the following steady-state temperature is established in the center of the beam at the surface of the target [2]:

$$T = \frac{Ir}{k} A + T_н, \tag{19}$$

where I is the radiation flux density; k is the thermal conductivity coefficient.

The presence of oscillations in the absorptivity in accordance with (19) should lead to an interesting effect: to jumps in the time of attaining the melting point $t_{пл}$ (I) at intensity values of:

$$I_s = k \frac{T_{пл} - T_н}{r A_{s\,max}}, \quad s = 1, 2, \ldots, \tag{20}$$

where $A_{s\,max}$ are the values of the absorptivity at the points of the interference maxima; $T_{пл}$ is the melting point.

In fact, with a reduction in the intensity I from a value of $I_s + \delta I$ down to a value of $I_s - \delta I$, it is necessary to increase the oxide film by the amount $\Delta x \approx \pi/\beta$, where the requisite value of the absorptivity is chosen anew (see Figure 1). The jump in the heating time $\Delta t_{тл}(I_s)$ is equal to the time needed to build up the oxide film by the thickness of approximately Δx. We have from (1), (19), and (20):

$$\Delta t_{пл}(I_s) = \frac{1}{d} \int_{x_{s\,max}}^{x_s} x \exp\left\{ \frac{T_д}{(T_{пл} - T_н) A(x)/A_{s\,max} + T_н} \right\} dx, \tag{21}$$

where $x_{S\ max}$ is the position of the maximum of the function $A(x)$; x_S is the root of the equation $A(x_S) = A_{S\ max}$ closest to $x_{S\ max}$.

To estimate the size of the jump $\Delta t_{пл}$ in (21), one can assume $A(x) \approx A_{S\ max} = \text{const}$, so that:

$$\Delta t_{пл} \sim \frac{(x_s - x_{s\,max})^2}{2d} \exp\left(\frac{T_л}{T_{пл}}\right). \qquad (22)$$

We will note yet one more effect which should be observed when heating massive samples. Since according to equation (1), the fastest growth in the oxide film occurs at those points where the surface temperature is maximum, then the absorptivity of the system also changes the most rapidly at these same points. For this reason, heating a metal in an oxidizing atmosphere should be accompanied in the initial stage of the activation process by a sharpening of the spatial temperature profile.

6. The Experimental Procedure

We conducted experimental studies of the process of heating metal in air subject to the action of the continuous radiation of a CO_2 laser. Copper plates with dimensions of approximately 3 x 3 mm and a thickness of approximately 1 mm were used as the targets.

The change in the target temperature was recorded with a chromel-copel or a chromel-alumel thermocouple, which was caulked into the back of the target, approximately in its center. The signal was fed from the thermocouple to the input of an N-115 bifilar suspension oscillograph, with which the time-wise curve of the target temperature $T(t)$ was recorded during its heating. The diameter of the radiation zone on the target was 1-2 mm, and the heating time varied from a few seconds up to several minutes. Under these conditions, a copper plate can be treated as thermally thin.

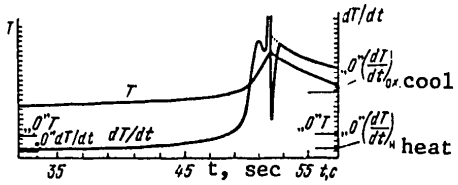

Figure 5. A section of an experimental oscillogram of the oxidation of copper in air at P = 21 w, m = 50 mg and A_0 = 2%.

The scale divisions along the ordinate for the T signal are equal to 23.3°, and for the dT/dt signal are 16.4° deg/sec. Shown in the right part of the oscillogram are the cooling

[Notes to Figure 5 continued]:

curves. The point in time t = 51.5 sec corresponds to the termination of the radiation. At this point in time, the polarity of the dT/dt signal reversed, because of which, the position of its zero point also changed.

* * *

A dT/dt signal, which was formed by means of a differentiating RC network with a time constant $\tau = 0.02$ sec, was fed to the input of the bifilar oscillographs simultaneously with the T(t) signal. Both of these signals were also recorded following the termination of radiation (cooling curves), something which made it possible to strictly account for thermal losses and determine the true function A(T) (see Figure 2). In fact, during target heating, taking thermal losses into account, the dP/dt signal is described by expressions (11) and (12), while following the termination of the laser pulse, the following signal is picked off from the RC network:

$$\frac{dT}{dt} = -\frac{P_{\text{пот}}(T)}{mc_0}. \tag{23}$$

Subtracting (12) and (23) from each other for the case of an identical value of the temperature on the heating and cooling curves, we obtain:

$$A(T) = \frac{mc_0}{P}\left[\left.\frac{dT}{dt}\right|_{\text{нагр}} - \left.\frac{dT}{dt}\right|_{\text{охл}}\right]. \tag{24}$$

[нагр = heating; охл = cooling]

A typical experimental oscillogram is shown in Figure 5.

The T(t) signal was calibrated in two ways: based on the target heating in water in a temperature range of 20--50° C, and based on the known value of the melting point of copper of $T_{\text{пл}} = 1{,}080°$ C. Both of these methods yield close values for the temperature scale on the oscillograms, something which is characterized by a high linearity of the temperature scale in a range of 0--1,100° C. The dT/dt signal was calibrated by means of recording the "cold" T(t) and dT/dt curves for heating the target by 20--30° C. In this case, the influence of thermal losses can be neglected, and the target temperature varies linearly in time, in accordance with the law:

$$T = \frac{PA_0}{mc_0}t + T_{\text{н}}.$$

In this case, the value of the jump in the initial section of the dT/dt curve is equal to $PA_0/(mc_0)$, something which makes the requisite calibration possible.

The experimental results are in good agreement with the theoretical concepts set forth above.

We will note that a decrease in the absorptivity is usually observed in experiments on plates with a large value of A_0 in the initial heating section. This is related to the annealing of the target and the removal of micro-impurities from it, i.e., to laser "cleaning" of the surface [7, 12].

It should be underscored in conclusion that the oxidizing reactions which occur with the action of laser radiation on the surface of metal reflectors can lead to a marked degredation of their reflective characteristics.

BIBLIOGRAPHY

1. J.F. Asmus, F.S. Baker, "Rec. of 10th Symp. Electron. Ion. Laser Beam Techn.", 1969, p 241.

2. V.L. Volod'kina, M.N. Libenson, V.G. Prokopenko, L.A. Surmenko, "Rezka tonkosloynykh materialov izlucheniyem CO_2-lazera" ["Cutting Thin Layer Materials with CO_2 Laser Radiation"], Leningrad, LDNTP [Leningrad Scientific and Technical Popularization House], 1973.

3. V.L. Volod'kina, K.N. Krylov, M.N. Libenson, FIZIKA I KHIMIYA OBRABOTKI MATERIALOV [PHYSICS AND CHEMISTRY OF MATERIALS PROCESSING], No 5, 145, (1975).

4. V.P. Veyko, G.A. Kotov, M.N. Libenson, M.N. Nikitin, DAN SSSR [REPORTS OF THE USSR ACADEMY OF SCIENCES], 208, 587 (1973).

5. N.N. Rykalin, A.A. Uglov, A.N. Kokora, FIZIKA I KHIMIYA OBRABOTKI MATERIALOV, No 3, 3 (1974).

6. M.I. Arzuov, A.I. Barchukov, F.V. Bunkin, V.I. Konov, A.A. Lyubin, KVANTOVAYA ELEKTRONIKA [QUANTUM ELECTRONICS], 2, 1717, (1975).

7. M.I. Arzuov, V.I. Konov, S.M. Mwrwc, [illegible]. Silenok, N.I. Chapliyev, Preprint FIAN [Physics Institute of the USSR Academy of Sciences imeni P.N. Lebedev Preprint], Moscow, 1977, No 152.

8. "Thermophysical Properties of Matter", "The TPRS Data Series", Vol 8, N.Y., 1972.

9. O. Kubashevskiy, B. Gopkins, "Okisleniye metallov i splavov" ["The Oxidation of Metals and Alloys"], Moscow, Metallurgiya Publishers, 1965.

10. L.D. Landau, Ye.M. Lifshits, "Elektrodinamika sploshnykh sred" ["The Electrodynamics of Continuous Media"], Moscow, GITTL, 1957.

11. M.I. Arzuov, F.V. Bunkin, N.A. Kirichenko, V.I. Konov, B.S. Luk'yanchuk, PIS'MA V ZHETF [LETTERS TO THE JOURNAL OF EXPERIMENTAL AND THEORETICAL PHYSICS], 27, 230, (1978).

12. M.I. Arzuov, F.V. Bunkin, N.A. Kirichenko, V.I. Konov, B.S. Luk'yanchuk, Preprint FIAN, Moscow, 1978, No 39.

8225
CSO:8144/1216

QUANTUM ELECTRONICS

UDC 621.378.33

AN EXPERIMENTAL INVESTIGATION OF A METHOD OF CONTROLLING THE RADIATION PULSE WAVEFORM OF A CO_2 AMPLIFIER

Moscow KAVANTOVAYA ELEKTRONIKA in Russian Vol 6 No 3, 1979 pp 513-517

[Article by V.V. Makoimov, A.M. Orishich, L.M. Pakhomov and A.G. Ponomarenko, Institute of Theoretical and Applied Mechanics of the Siberian Department of the USSR Academy of Sciences, Novosibirsk, manuscript received 5 May 78]

[Text] A method of controlling the waveform and width of the radiation pulse generated in a CO_2 amplifier system, for the case of fast excitation of the active medium, based on the difference in the energy release times from the oscillatory states of CO_2 and N_2, was experimentally studied for the first time. Control of the pulse waveform was achieved by varying the delay time τ_d between the onset of excitation of the optically active medium of the amplifier and the moment of radiation injection of the master oscillator. The width of the output signal varied within limits of 0.06—2 μsec, where the amplifier efficiency was practically constant at ≈ 10%. It was demonstrated that the maximum pulse compression under the conditions of this experiment was limited to a time of ≈ 60 nsec, something which is apparently related to the finite rise time of the master oscillator pulse and the energy relaxation processes from the oscillatory and rotational states of CO_2 molecules in the active medium.

The practical utilization of high power laser systems depends a great deal on the capability of controlling the radiation pulse waveform. The generation of pulses with a width of equal to or greater than 1 μsec is required in lidars, communications, holography, as well as in various physical and chemical and biological investigations. Shortening the width of the radiation pulses, and especially, increasing the rise time, are necessary for better amlification of the light pulses in laser amplifiers and the high temperature heating of a plasma [1]. For this reason, studies of ways of controlling pulse width while retaining the high efficiency of a CO_2 amplifier system are of particular interest.

A method of controlling the waveform and width of a pulse, produced in a CO_2 amplifier system, is studied experimentally for the first time in this paper, for the case of fast excitation of the optically active medium, based on the difference in the times of energy release from the oscillatory states of CO_2 and N_2. Numerical modeling of such an amplification mode was carried out in paper [2].

The basic configuration of the setup is shown in Figure 1. A TEA CO_2 laser 1, operating at the P (20) transition, was used as the master oscillator. A detailed description of it is given in [3]. The optical resonator of the laser was formed by spherical metal mirror 2 with a radius of curvature of R = 10 m, and plane parallel plate 3 made of KRS-5. The radiation pulse waveform is also shown in Figure 1. Approximately 20% of all the radiation energy was contained in the initial short peak (see curve 1 in FIugre 2e) with a half-height width of ≈70 nsec.

High power electrical ionization system 8 which is described in detail in paper [4], was used as the amplifier. The optically active medium was produced within about 0.5 μsec in a volume of 10 x 10 x 100 cm, filled with a mixture of commerically pure CO_2 and N_2 gases at a pressure of 1 atm. The average value of E/p, at which the energy was absorbed, amounted to about 10 V/(cm · mm Hg).

A dual path configuration was employed for modeling the two meter amplifier. The radiation beam of the master oscillator was passed through the optically active medium by means of spherical mirrors 6, 7, and 10-12 (see Figure 1), and in this case, it was compressed to increase the energy flux density. The average cross-section of the laser beam amounted to ≈ 5 cm^2. Window 9, made of BaF_2, was used for the radiation input and output. Although we took special precautions to prevent self-excitation of the amplifier using optical elements, the influence of the amplifier on the radiation pulse waveform of the master oscillator was nonetheless observed at an absorbed energy density of ≈ 0.2 J/(cm^3 · atm).

To record the master oscillator and amplifier pulse energies, part of the energy was split off by means of dividing plates, 4, 14, 21 and steel reflector 13 to TPI-2-5 standard calorimeters (17, 24). Specially designed recorders 16 and 23, based on the effect of entraining the charge carriers in the semiconductors with photons [5], with radioelectronic amplifiers 18 and 25, were employed to measure the absolute power and waveform of the pulses. The signal from the master oscillator pulse waveform recorder was registered on the S1-11 oscillograph (26), and that from the radiation amplifier on the S7-10A (19) and the S1-11 (20) oscillographs in such a fashion that the "traveling wave" type deflecting system of the S7-10A oscillograph was series loaded into the S1-11 oscillograph. By setting the different sweep rates and sensitivities, as well as the calibration attenuators made of teflon flim, 5, 15, and 22, it was possible to observe a short peak in detail on one oscillograph, and on the other, the gently sloping decay of the radiation pulses without losses in the amplitude of the signals being measured.

The delay time between the start of excitation of the optically active medium of the amplifier and the master oscillator radiation pulse was recorded by a dual trace S8-2 oscilloscope (27). At the same time, the power characteristics of the volumetric discharges of the amplifier and the master oscillator were monitored in the experiment by means of OK-21 oscilloscopes (28, 29).

The errors in measuring the amplitude of the electrical signals and the time intervals did not exceed 10%. The time resolution of the recorders, which was determined experimentally, amounted to 3 nsec.

The absolute calibration of the recorder sensitivity in conjunction with the measurement channel was accomplished directly in the operating optical circuit. The pulse of a TEA laser, operating with pure CO_2 and generating radiation with a width of $\approx$ 100 nsec, was employed for these purposes. The error in the absolute calibration should not exceed 20%.

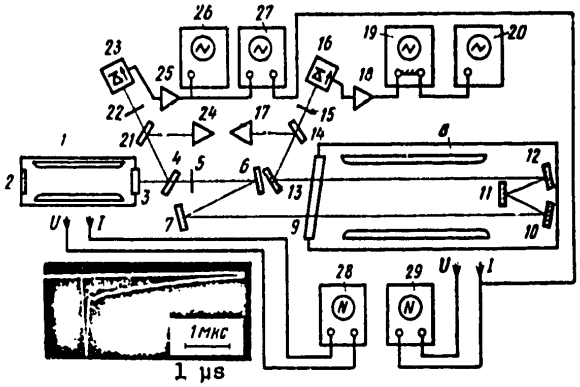

Figure 1. Basic schematic of the setup, and the master oscillator radiation pulse waveform.

The dynamic gain of the optically active medium was measured using a probe signal method with a low power, $I_{r0} \approx 1$ watt. A CW laser with an optical shutter, operating at the P (20) transition was employed in these experiments as the master oscillator.

A typical curve for the timewise change in the gain α is shown in Figure 2a. It can be seen from the resulting curve that for the case of fast pulse excitation (< 0.5 μsec) of the optically active medium, more than 80% of the energy is stored in the N_2 oscillations, and then during $\approx$ 1.5 μsec equilibrium is established between the N_2 and the asymmetric CO_2 mode, and in this case, α increases. Curves of the intensity as a function of time for a radiation pulse I_r at the output of the amplifier for the case of various delays τ_d between the onset of excitation of the optically active medium and the point in time of the injection of the oscillator radiation pulse

I_{r0} into the amplifier are shown in Figures 2b-2d. The parameters of the oscillator pulse were practically the same for all modes, and the power density at the maximum for an unamplified signal was $I_{r0}^{max} \approx 1.4$ MW/cm^2. When $\tau_d < 100$ nsec, a quasisteady-state mode is of energy output is formed with a characteristic time of ≈ 2 μsec (see Figure 2b). Increasing τ_d leads to a reduction in the total pulse width and the appearance of an initial high power peak (see Figures 2c, 2d), in which more than half of the pulse energy is liberated when $\tau_d > 1$ μsec.

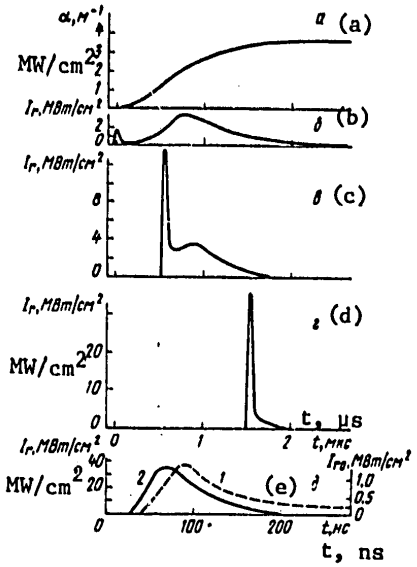

Figure 2. The small signal gain α (a) and the amplified signal power as a function of time for delays $\tau_d = -0.05$ μsec (b), 0.5 μsec (c) and 1.5 μsec (d), as well as the peak power at the output of the amplifier in the absence of I_{r0} (1) and in the presence of the optically active medium I_r (2) where $\tau_d = 1.2$ μsec (e).

The mixture of gases CO_2:N_2 = 1:2, the total pressure was 1 atm, and the specific absorbed energy density was Q/p = = 0.16 J/(cm^3 · atm).

The ratio of the energy Q_{r1} radiated at the peak of a power of $I_r \geq 0.5\ I_r^{max}$, to the total radiation pulse energy at the output of the amplifier, Q_r, is shown in Figure 3a as a function of the absorbed energy density for various partial pressures of the CO_2 and N_2 gases and $\tau_d = 1.2$ μsec. The size of Q_{r1} was determined by numerical integration of the oscillograms of the radiation pulses. It can be seen from the results that with an increase in the CO_2 partial pressure, the fraction of the energy in the initial high power peak reaches 80%. It is significant that when the overall pulse width of the master oscillator was about 3 μsec, its gain when $\tau_d > 1$ μsec was practically terminated about 200 nsec after the signal was fed in, and despite the fact that the small signal gain reached about $3 \cdot 10^3$, the ratio of I_r^{max}/I_{r0}^{max} was less than 30 for all cases. Thus, in the given mode, the energy and power of only the initial peak of the oscillator pulse were amplified.

It is essential to note that we did not study the possibility of obtaining maximum efficiency of the amplifier system. The efficiency of the amplifier,

estimated using the expression $\eta = (Q_{out} - Q_{in})/Q_p$ (Q_{out} and Q_{in} are the output and input energy of the amplifier; $Q_p = Q_0 V_1/V_0$; Q_0 is the total energy absorbed in the discharge having a volume V_0; V_1 is the volume through which the radiation passes), did not depend on τ_d and amounted to about 10%. It is necessary to note that with changes in the manner of tapping the energy, the amplifier efficiency practically did not change.

The mode of energy liberation from the optically acive medium for the case of fast pulse excitation is determined both by the parameters of the radiation pulse being amplified and by the collision processes which lead to the population of the upper lasing level and the depletion of the lower lasing level. Since the transfer time for the N_2 oscillation energy to the CO_2 asymmetrical mode and for the deactivation of the lower lasing level under the conditions of our experiment were substantially greater than the times for rotational and intramodal oscillatory relaxation [6], specifically the first two processes were responsible for the quasisteady-state energy mode for the case of small delays τ_d and oscillator radiation intensities of $I_{r0} >> h\nu/(\sigma\tau_{34})$ (where σ is the stimulated trasition cross-section; τ_{34} is the transfer time for energy from the N_2 to the asymmetrical CO_2 mode; $h\nu$ is the energy of a radiation quantum).

If the oscillator radiation pulse is injected into the amlifier when $\tau_d > 1$ μsec, then the major part of the absorbed energy is stored in the asymmetrical oscillations (especially in a gas mixture with a large partial content of CO_2), something which permits shaping the short radiation peak at the amplifier output, where the width of the peak can be determined by both the rotational and intramodal oscillatory relaxation times and the waveform of the oscillator radiation pulse.

The study of the maximum energy output rate from the amplifier while maintaining its high efficiency was of particular interest. The deformation of the initial peak of the master oscillator pulse was studied when it passed through the two meter amplifier. The input signal energy flux with a width of about 70 nsec amounted to 0.1 -- 0.2 J/cm^2.

Typical curves for the power density at the maximum I_r^{max} and the half-height peak width Δt for the radiation pulse at the amplifier output are shown in Figures 3b and 3c as a function of the absorbed energy density Q/p. It can be seen from the data presented that the pulse power increases with an increase in the injected energy: $I_r^{max} \approx (Q/p)^{3/2}$, however, the peak width Δt practically does not change, despite the substantially the nonlinear gain.

It is well known [7] that if the master oscillator pulse has an exponentially rising leading edge, then when propagating in the optically active medium, its maximum experiences an additional shift "ahead", while the width can practically remain constant. In order to check the influence of this process under our experimental conditions, an additional investigation was made of the radiation pulse waveform distortion in the amplification process. To

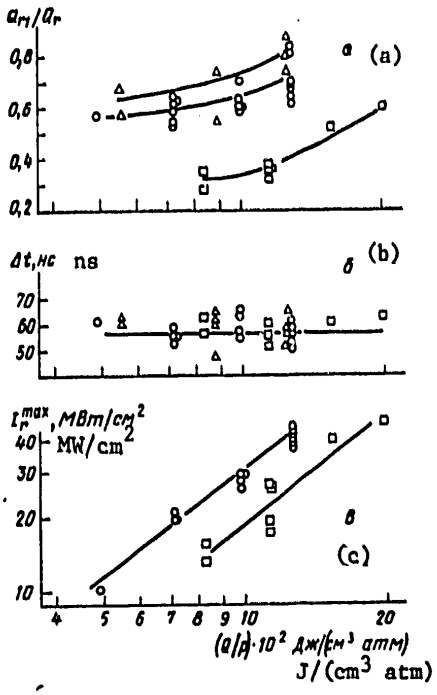

Figure 3. The fraction of the energy in the radiation pulse peak (a), the half-height pulse width (b) and the power density at the maximum radiation peak (c) as a function of the specific injected energy where τ_d = 1.2 μsec for mixtures of CO_2:N_2 = 1:2 (squares), 1:1 (circles) and 2:1 (triangles).

precisely measure the time of appearance of the pulse at the amplifier output relative to the start of the oscillator pulse, the signals from both recorders, decoupled in time, were fed to one beam of the S7-10A oscillograph.

Typical pulses at the output of the working chamber without gain (curve 1) and with gain (curve 2) are shown in Figure 2e. The shift "ahead" of the maximum of the intensity by 15—25 nsec was experimentally determined. On the other hand, as was demonstrated in papers [8, 9], the total energy rotational and intramodal oscillatory relaxation times to the specified oscillatory-rotational level for the case of a mixture pressure of 1 atm fall within a range of 1-10 and 20-70 nsec respectively, i.e., they are comparable with the width of the signal being amplified.

It can be assumed that under our experimental conditions, the limiting of the energy liberation rate of the optically active medium, found to have a characteristic time of ≈60 nsec, was due to both the finite width of the leading edge of the master oscillator pulse and the time for the rotational and oscillatory relaxation of the energy..

Thus, a simple and reliable method of controlling the waveform and width of a radiation pulse in a CO_2 amplifier system for the case of a constant excitation time of the optically active medium has been experimentally

investigated for the first time in this paper. The possibility of varying the energy release time in a range of 0,06--2 μsec at an efficiency of ≈ 10% has been demonstrated.

The authors are grateful to L.I. Loskutova for assisting in the processing of the results and V.N. Tishchenko for his useful discussions.

BIBLIOGRAPHY

1. V.A. Arsen'yev, I.N. Matveyev, N.D. Ustinov, KVANTOVAYA ELEKTRONIKA, 4, 2309, (1977).

2. A.G. Ponomarenko, V.N. Tishchenko, "Preprint ITPM SO AN SSSR" ["Preprint of the ITPM of the Siberian Department of the USSR Academy of Sciences"], Novosibirsk- 1978, No 1.

3. Yu.V. Afonin, A.M. Orishich, A.G. Ponomarenko, S.P. Shalamov, "Preprint ITPM SO AN SSSR", Novosibirsk, 1977, No 4.

4. A.M. Orishich, A.G. Ponomarenko, V.G. Posukh, R.I. Soloukhin, S.P. Shalamov, PIS'MA V ZHTF [LETTERS TO THE JOURNAL OF ENGINEERING PHYSICS], 3, 39, (1977).

5. L.M. Pakhomov, PTE [TECHNICAL OPERATION REGULATIONS], No 2, 252, (1976).

6. S.A. Trushin, V.V. Churakov, KVANTOVAYA ELEKTRONIKA, 4, 385, (1977).

7. P.G. Kryukov, V.S. Letokhov, UFN [PROGRESS IN THE PHYSICAL SCIENCES], 99, 169, (1969).

8. J.F. Figueira, W.H. Reichelt, G.T. Schappert, T.F. Stratton, S.A. Fenstermacher, APPL. PHYS. LETTS., 22, 216 (173).

9. R.J. Harrach, IEEE. J. QE-11, 349, (1975).

8225
CSO:8144/1216

QUANTUM ELECTRONICS

UDC 621.378.324

THE CHARACTERISTICS OF A CO_2 LASER EXCITED BY AN ALTERNATING CURRENT CAPACITIVE DISCHARGE

Moscow KVANTOVAYA ELEKTRONIKA in Russian Vol 6 No 3, 1979 pp 548-552

[Article by V.D. Gavrilyuk, A.F. Glova, V.S. Golubev, A.B. Kuznetsov, F.V. Lebedev and V.A. Feofilaktov, manuscript received 9 Jun 78]

[Text] A model of a steady-state fast flow CO_2 laser excited by an AC capacitive discharge at a frequency of 10 KHz was experimentally studied. The results of optimizing the laser operational modes are in agreement with the calculated results. In accordance with them, at the level of the specific pumping parameters achieved in operation, an industrial laser can be designed with a power of ≈ 20 KW with an overall efficiency of ≈ 15% and a specific radiation energy yield of ≈40-45 J/g.

1. The utilization of an alternating current capacitive discharge to pump gas lasers is of interest in connection with the prospects for dispensing with ballast resistors, as well as the simplification of the power supplies and the structural design of the discharge chamber. The possibility of creating a homogeneous alternating current discharge at a frequency of 10 KHz in a flow of N_2 with CO_2 added was shown in paper [1], and the feasibility of attaining specific mass energy contributions of $W_g \approx 300$–400 J/g at an overall oscillatory discharge efficiency of $\nu_{col} \approx 60\%$ was also demonstrated.

The results of experimental studies using a breadboarded fast flow CO_2 laser excited by a capacitive discharge, for the purpose of determining the efficiency of the conversion of the AC generator energy into radiation, optimizing the operational modes of the device and investigating the stability of the output radiation, are given in this paper.

2. The experimental setup of a fast flow CO_2 laser (Figure 1), consisted of a rectangular channel with a cross-section of 200 x 60 mm, through which the working mixture of gases (N_2, air, He, CO_2) was pumped. The gas velocity at the inlet to the discharge chamber was $v \approx 100$ m/sec, and the static pressure varied from 30 mm Hg. The transverse AC discharge at a frequency

of 10 KHz was realized between two flat dielectric plates, spaced $h \approx 60$ mm apart. The length of the discharge zone transverse to the flow amounted to 150 mm, and in the direction of the flow (L) varied from 180 to 390 mm. The discharge was powered with a motor-generator through a stepup transformer. A single-pass stable resonator, consisting of two copper reflectors with a diameter of 60 mm and radii of curvature of $R_1 = \infty$ and $R_2 = 600$ mm were placed in the downstream portion of the discharge zone. There was a through pole with a diameter of $d = 2$ mm, covered by a plate of NaCl, in the center of the flat reflector. The radiation absorption factor at the surface of the reflectors was determined by the method of multiple reflections and amounted to $r = 2 \pm 0.15\%$.

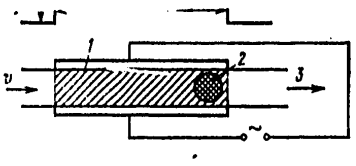

Figure 1. The experimental configuration:

Key: 1. The excitation zone (discharge zone);
2. Zone for registering the excitation (the resonator region);
3. Exhaust.

The conversion efficiency of the electrical energy to light energy was characterized by the electro-optical efficiency level, ν_{eo}, defined as the ratio of the radiation power absorbed in the reflectors of the resonator and brought out through the hole in the reflector, to the total electrical power consumed from the discharge power supply.

The tapped off radiation power, according to calorimetric measurements, did not exceed 5% of the power absorbed by the reflectors, and was proportional to it. In determining η_{eo} in this fashion, we did not take into account the radiation losses due to diffusion scattering at the reflectors, something which could lead to understating the size of η_{eo} by 10 - 15%. The total power consumption of the laser was determined from oscilloscope traces of the discharge and the voltage across the output terminals of the power supply. The spectra of the fluctuations in the discharge current and the radiation intensity were studied using a S4-12 spectrum analyzer, to the input of which a signal was fed from a metering shunt or from an FSG-22-3A1 transducer.

The calculation procedure we employed [2] allowed for the determination of the fraction of all of the oscillatory excited molecules, the energy of which is converted to stimulated radiation in the resonator (η_r), and the calculation of the system electro-optical efficiency η_{eo} as $\eta_{eo} = \eta_r \eta_k \eta_q$, where η_k is the oscillatory efficiency of the excitation method, while $\eta_q = 0.41$ is the quantum efficiency of the CO_2 laser. The calculations were performed for the case of the electro-optical configuration of the laser shown in Figure 1, in accordance with which the active medium is excited by a discharge which is uniform over the entire length of the zone L, while the excitation is registered in a resonator placed at the end of this zone, where the resonator is formed by two parallel reflectors with an absorption factor of r.

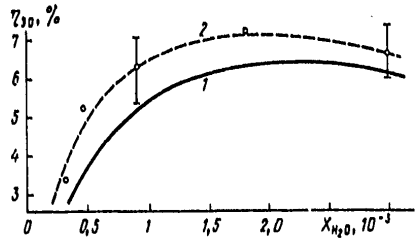

Figure 2. The theoretical (1) and experimental (2) curves for η_{eo} as a function of the water concentration at p = 30 mm Hg, v ≈ 100 m/sec, jE ≈ 4.1 (1) and 4.5 (2), $X_{CO_2} = 6 \cdot 10^{-2}$, L = 180 mm (1) and 190 mm (2), X_{H_2O} was assured by the air feed.

Results of experiments to estimate the energy balance in an AC discharge were employed in the calculations [1], i.e., it was assumed that 60% of the power supply energy goes to excite the oscillatory levels of the nitrogen molecules, 25% to direct heating of the gas, while the remaining 15% is expended in heating the electrodes and structures, exciting the electron levels, ionization, plasma-chemical reactions and other processes.

4. The basic results were obtained when using a helium free operating mixture, consisting of commercially pure nitrogen (O_2 content up to 2-3%), CO_2 and air at a total pressure of 30 mm Hg. The air rate of flow delivered water to the discharge chamber having a molar content of $X_{H_2O} \approx (0.005\text{-}0.5)X_{CO_2}$. The quantity X_{CO_2} was varied within a range of 0.01 - 0.1. Individual measurements were also taken with a mixture of N_2 and He in a molar ratio of 1:1 with CO_2 added.

The discharge was visually homogeneous in practically all operational modes. The maximal achieved values of the volumetric energy contribution $\overline{jE}$ did not exceed 4.5 watts/cm^2 and were limited by the power supply and the size of the ballast capacitance of the electrode elements. The level of the specific mass energy contribution achieved 150 J/g at L ≈ 190 mm and 280 J/g at L ≈ 390 mm. The generation threshold, depending on X_{CO_2} was reached at $(jE)_{thr} \approx 0.5\text{-}1.5$ watts/cm^3. The generation power depended jE, and also on the X_{CO_2} and X_{H_2O} in the mixture. As can be seen from the curves in Figure 2, η_{eo} increases rapidly with an increase in X_{H_2O} up to $(0.01\text{-}0.02)X_{CO_2}$, and thereafter is saturated, however, when $X_{H_2O} \approx (0.03\text{-}0.04)X_{CO_2}$ visually observable inhomogeneities [3] appear in the plasma, and for this reason, the optimal water content is $X_{H_2O}^{opt} \approx (0.02\text{-}0.03)X_{CO_2}$.

The optimum CO_2 content falls in a range of 4-7%. With optimum H_2O contents, the size of η_{eo} increases sharply with an increase in jE within a range of $(1\text{-}2)\ (jE)_{thr}$, and thereafter remains at a constant level. Typical results of optimizing X_{CO_2} for helium mixtures (X_{N_2}:X_{He} = 1:1) for various discharge chamber lengths L are shown in Figure 3. They are similar in nature to the function $\eta_{eo} = f(X_{CO_2})$ for the case of $X_{He} = 0$.

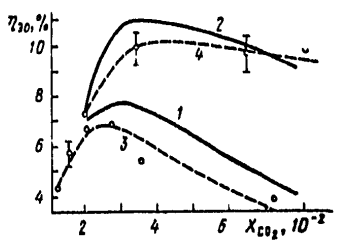

Figure 3. The theoretical (1,2) and experimental (3,4) curves for η_{eo} as a function of X_{CO_2} (for a helium mixture of $X_{N_2}:X_{He}$ = 1:1 where p = 50 mm Hg, v = = 100 m/sec; jE = 4.1 (1,2), 3.2 (3) and 3.0 (4) watts/cm^3; L = 360 mm (1), 180 mm (2), 390 mm (3) and 190 mm (4).

5. The computed curves for η_{eo} = = $f(X_{H_2O}; X_{CO_2}; L)$ shown with the solid lines in Figures 2 and 3 are in good agreement with the experimental results, something which allows the application of this calculation procedure [2] to the estimation of the efficiency of employing an AC discharge for pumping CO_2 lasers, as well as for optimization of the operational modes of such a laser according to the composition of the mixture, the dimensions of the gas discharge chamber and the resonator transmittance.

We carried out such an optimization calculation for the total efficiency, η, for a typical variant [4, 5] of an industrial, fast flow CO_2 laser with a discharge chamber length in the direction of the flow of L = 40 cm, a height of 6 cm, and a width (along the optical axis) of about 1.5 m, which was equipped with a fully integrated resonator, consisting of reflectors with r = 2%. In this case, the quantity η was defined as the fraction of the energy consumed from the power supply, transformed into stimulated radiation and brought out of the laser resonator. According to the results obtained at v = 100 m/sec, p = 50 mm Hg, jE = 4 W/cm^3, and when a mixture of He and N_2 (in a molar ratio of 1:1) with CO_2 added (X_{CO_2} = 0.06) was used as the working medium at the input to the discharge chamber, the value of η attained 14-15%, which corresponds to an output radiation power of ≈ 20 KW. The magnitude of the specific energy yield in this case amounts to about 40-45 J/g.

By using an independent DC discharge to excite the medium, for the case of similar mass rates of gas flow and geometric parameters of the setup [4,6], only from 5 to 9% of the energy consumed from the power supply can successfully be changes to stimulated radiation. The basic possibility of achieving a specific energy yield of 20-40 J/g in a laser with similar parameters, when the medium is excited with a transverse combination discharge with a gap of 10 cm and L = 15 cm is indicated in paper [7]. The cited values of the specific and output characteristics permit the assumption that AC discharge is an extremely efficient method of pumping CO_2 lasers.

6. In analyzing the model's radiation fluctuation spectrum, which is shown in Figure 4a, it is necessary to segregate the fluctuations at a frequency of 20 KHz, which correspond to the oscillations of the exciting discharge current (f = 10 KHz), and the "lower frequency" oscillations, the spectrum of which

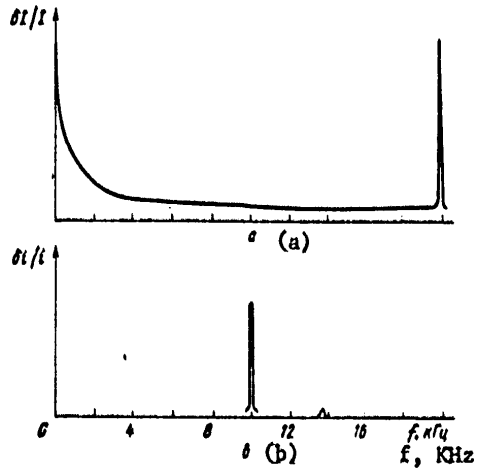

Figure 4. The frequency spectra of the radiation (a) and the discharge current (b).

fills the range of frequencies from about 10^2 Hz up to several kilohertz, while the maximal amplitude is comparable to the amplitude corresponding to the primary frequency. The modulation level of the radiation amounted to 3-5% at f ≈ 20 KHz.

A comparison of the spectra of the fluctuation of the radiation and current (Figure 4b) permits the hypothesis that the low frequency fluctuations are not related to the discharge, and are possibly caused by mechanical oscillations of the reflectors of the resonator due to the vibration of the setup, since each of them is secured to the housing of the chamber independently and no special measures were taken to counter relative motions of the reflectors.

The modulation of the radiation at f = 20 KHz was caused by fluctuations in the power liberated in the discharge, and for the case of a fully incorporated resonator, its level under our conditions should amount to:

$$\approx \frac{1}{2f\tau_{rel}}\left(1+\frac{\tau_{rel}}{\tau_{stim}}\right) \approx 10^{-2} - 10^{-1}$$

(τ_{rel} is the time for the collision relaxation of the energy stored in the oscillatory degrees of freedom; $\tau_{stim} \approx (10^{-1} - 1) \cdot \tau_{rel}$ is the characteristic

stimulated radiation time), which is in agreement with the experiment. Such modulation is not dangerous when using a laser for industrial purposes and can in principle be reduced when the excitation frequency is increased. It is necessary to note that under our conditions, the oscillation described in [8] in a range of 3 - 20 KHz, as well as oscillations at transit frequencies of $\nu_{trans} \approx v/R \approx 3$ KHz, where R is the radius of the oscillation region, were not observed.

7. The results of the experiments and calculations presented in this paper make it possible to come to the following conclusions:

1) An AC discharge at a frequency of 10 KHz is an effective method of exciting the medium of CO_2 laser, which permits a substantial simplification of the structural design problems and power supply problems, as well as allows for the creation of a simple industrial CO_2 laser with a power of $\approx$ 20 KW with an overall conversion efficiency of $\approx$ 15% and a specific energy yield of 40-45 J/g;

2) The fluctuations in the radiation related to the method of excitation do not exceed a few percent, and can in principle be decreased;

3) The method used for modeling a laser by means of a "dead end" resonator in conjunction with the calculations allows for the investigation of the specific characteristics of the radiation, the estimation of the efficiency of an actual laser, and can be useful in studying the efficiency of pumping fast flow gas discharge lasers using prototypes with a small optical access length.

BIBLIOGRAPHY

1. V.D. Gavrilyuk, A.F. Glova, V.S. Golubev, F.V. Lebedev, KVANTOVAYA ELEKTRONIKA, 4, 2034, (1977).

2. B.F. Gordiyets, A.I. Osipov, Ye.V. Stupenchenko, L.A. Shelepin, UFN [PROGRESS IN THE PHYSICAL SCIENCES], 108, 655, (1972).

3. A.F. Glova, V.S. Golubev, A.Ye. Katomin, F.V. Lebedev, FIZIKA PLAZMY [PLASMA PHYSICS], 3, 1396, (1977).

4. F.K. Kosyrev, N.P. Kosyreva, Ye.I. Lunev, AVTOMATICHESKAYA SVARKA [AUTOMATIC WELDING], No 9, 72, (1976).

5. S.O. Brown, J.W. Davis, APPL. PHYS. LETTS., 21, 480, (1972).

6. A.V. Artamonova, et al., KVANTOVAYA ELEKTRONIKA, 5, 920, (1978).

7. A.P. Napartovich, V.G. Naumov, V.M. Shashkov, PIS'MA V ZHETF [LETTERS TO THE JOURNAL OF EXPERIMENTAL AND ENGINEERING PHYSICS], 3, 349, (1977).

8. A.V. Artamonov, V.G. Naumov, KVANTOVAYA ELEKTRONIKA, 4, 178, (1977).

8225
CSO:8144/1216

QUANTUM ELECTRONICS

UDC 535.375.5

LETTERS TO THE EDITOR OF QUANTUM ELECTRONICS

Moscow KVANTOVAYA ELEKTRONIKA in Russian Vol 6 No 3, 1979 pp 592-593

[Letter by B.Ya. Zel'dovich, I.G. Zubarev, G.A. Pasmanik and V.G. Sidorovich, received 21 Jun 78; reply by V. Gerasimov, received 19 Jul 78]

[Text] Concerning the Papers of V.B. Gerasimov and Coauthors

Articles by V.B. Gerasimov and his coauthors, devoted to certain aspects of VKR and VRMB [expansions unknown], were recently published in the journal KVANTOVAYA ELEKTRONIKA. Unsubstantiated assertions, as well as explicit errors are found in a number of these papers. Correct theoretical concepts of the operation of stimulated scattering lasers and concerning the inversion of the wave front for the case of VRMB are nonetheless especially needed at the present time in connection with the fact that several practical applications have been noted for these transducers, the design of which is engaging an increasing number of experimenters.

We shall consider the three latest publications. The incorrect assertion that when wideband, spatially incoherent pumping is used, the selective properties of a VRMB reflector increase significantly, was advanced in paper [1]. In actual fact though, the strictional force causing the amplification of the hypersonic waves, is given by the expression $f \approx E_H E_S$, and for this reason, with the inversion of the wave front, when $E_S \propto E_H$, we obtain $f \propto E_H^2$. It follows from this that the hypersound intensity, other conditions being equal, attenuates with a pumping spectrum width $\Delta\nu_H$, which considerably exceeds the line width of spontaneous Mandel'shtam-Brillouin scattering, $\Delta\nu_{sp}$ (by $\Delta\nu_H\Delta\nu_{sp}$ times). The stokes wave increment also falls off just as many times (including that reproducing the pumping). Consequently, the selective properties of a VRMB reflector do not increase with an increase in $\Delta\nu_H$.

It is likewise asserted in this paper that the selective properties increase when the path length of the accoustic wave l_{aw} is greater than the diffraction intermixing length of the radiation $l_d = \lambda/\theta_H^2$. This assertion is not based on anything and is in error.

Paper [2] speaks of an "acoustic" reflector with a plane wave front of acoustic phonons. However, such a reflector reflects light just as a conventional flat reflector and it does not make sense to compare it with a VRMB reflector, which inverts the wave front (in the latter case, with a sufficiently high attenuation of the hypersound, its wave front reproduces the pumping wave front).

In paper [3], based on the previous works of V.B.Gerasimov, including those considered above, the same errors are repeated and unsubstantiated and false conclusions are drawn concerning the operation of a VRMB laser.

P.S.: We were acquainted with the reply of V.B. Gerasimov to our letter, which is published below, and in our opinion, no proven positive assertions are contained in this reply.

BIBLIOGRAPHY

1. V.B. Gerasimov, S.A. Gerasimova, V.K. Orlov, "O znachitel'nom uvelichenii selektiruyushchikh svoystv VRMB zerkala" ["On a Significant Increase in the Selective Properties of a VRMB Reflector"], KVANTOVAYA ELEKTRONIKA, 4, No 4, 932 (1977).

2. V.B. Gerasimov, V.K. Orlov, "Vosproizvedeniye volnovykh frontov pri rasseyanii sveta na akusticheskikh volnakh i dinamicheskaya golografiya" ["The Reproduction of Wave Fronts with Light Scattering at Acoustic Waves, and Dynamic Holography"], KVANTOVAYA ELEKTRONIKA, 5, No 2, 436 (1978).

3. V.B. Gerasimov, V.K. Orlov, "O vliyanii effekta obrashcheniya volnovykh frontov na rabotu VRMB-lazera" ["On the Influence of the Wave Front Inversion Effect on the Operation of a VRMB Laser"], KVANTOVAYA ELEKTRONIKA, 5, No 4, 906 (1978).

Reply to the Letter to the Editor of B.Ya. Zel'dovich, I.G. Zubarev, G.A. Pasmanik and V.G. Sidorovich

In the papers considered in the letter, dealing with the analysis of stimulated back scattering (VRN) of wideband laser radiation, we proceeded from the equations [1]:

$$\hat{L}E_r = i\gamma_r X^* E_1 ; \qquad \hat{L}E_1 = i\gamma_1 X E_r, \tag{1}$$

erroneously assuming that when the condition $L < 1/\Delta\nu_H$ is met (where L is the effective scattering length; $\Delta\nu_H$ is the pumping spectral width), the form of the operator $\hat{L}$ is the same both for the pumping field and for the

back scattered radiation. B.Ya. Zel'dovich pointed this error out to the authors following the publication of papers [1-3].

An analysis of equations (1) led to the erroneous conclusion for VRN, that in the process of scattering wideband radiation into a component with an inverted wave front, a predominantly plane, monochromatic hypersonic wave is excited in the medium (something which, however, is justified for foreward scatter, for example, for a wave of optical phonons in the case of VKR [1]). This result generated other erroneous results, which were noted in the letter: the conclusion that the selective properties of a VRMB reflector increased when using wideband pumping and pumping, the radiation intermixing diffraction length of which is less than the acoustic wave path length [2], as well as the conclusion of the possibility of inverting a wave front at a plane acoustical wave [1]. (The conclusion concerning the possbility of reproducing a wave front at a plane wave of optical phonons in the case of VKR remains valid.)

An erroneous result concerning the gain increment of the component with the inverted wave front [2] was used in paper [3] in analyzing the VRMB generator. However, we will note that if this erroneous result is replaced by the correct one, in accordance with which the gain increment of the mirror reflected component is $\Delta\nu_H/\Delta\nu_{ak}$ times greater than the gain increment of the laser mode, then the results of paper [3] remain valid. It should be noted that the VRN pumping mode, which cannot be represented in the form $\phi_H(r,z)\phi(\eta)$ (see [4]) under the conditions $L \ll 1/\Delta\nu_H\Delta\nu_{ak} \ll \Delta\nu_H$ and $L \gg \lambda/\theta_H^2$, was not considered prior to our papers [1-3] for after them (see [4]).

The conclusion concerning the predominant excitation of a monochromatic hypersonic wave in the case of scattering of wideband radiation under the conditions we indicated [1-3] remains valid, if scattering into the mirror reflected component is considered.

On behalf of the authors of papers [1-3], V. Gerasimov.

BIBLIOGRAPHY

1. V.B. Gerasimov, V.K. Orlov, KVANTOVAYA ELEKTRONIKA, 5, No 2, 436 (1978).

2. V.B. Gerasimov, S.A. Gerasimova, V.K. Orlov, KVANTOVAYA ELEKTRONIKA, 4, No 4, 932 (1977).

3. V.B. Gerasimov, V.K. Orlov, KVANTOVAYA ELEKTRONIKA, 5, No 4, 906 (1978).

4. G.A. Pasmanik, PIS'MA V ZHTF [LETTERS TO THE JOURNAL OF ENGINEERING PHYSICS], 4, No 9, 504 (1978).

8225
CSO:8144/1216

QUANTUM ELECTRONICS

UDC 621.373.826.038.823

A COMPACT PERIODIC PULSED CO_2 LASER

Moscow KVANTOVAYA ELEKTRONIKA in Russian Vol 6 No 3, 1979 pp 597-598

[Article by M.I. Arzuov, S.K. Vartapetov, M.Ye. Karasev, V.I. Konov and V.V. Kostin, Physics Institute imeni P.N. Lebedev of the USSR Academy of Sciences, Moscow, manuscript received 28 Jul 78]

[Text] The construction of a laboratory CO_2 laser is described having a pulse repetition rate of f ≈ 350 Hz and an average power P of up to 80 watts for a half-height pulse width of ≈ 3 μsec. The average power is studied as a function of f, as well as the timewise stability of P. For the case of continuous operation at a frequency of 100 Hz, without renewing the gas mixture for a period of 30 minutes, the average radiation power falls off by no more than 15%. It is shown that discharge contraction occurs not because of overheating of the mixture, but as a result of its chemical decomposition.

Atmospheric pressure CO_2 lasers with a high pulse repetition rate have lately been attracting increasing attention. On one hand, such lasers make it possible to obtain high average radiation power levels, comparable to CW CO_2 lasers, and on the other hand, high peak radiation powers characteristic of pulsed TEA lasers. These properties make periodic pulsed CO_2 lasers extremely promising for physics research and for industrial application.

To obtain a uniform discharge in each pulse, it is necessary to prevent excess heating of the gas by the scattered pumping energy. When the excess heat is diverted to the walls solely by virtue of the heat conductivity of the mechanism, the maximum pulse repetition rate does not exceed 30-50 Hz, something which limits the average radiation power [1]. However, this limitation can be removed if fast pumping of the gas mixture through the discharge region is employed [2]. The most convenient configuration is that where the direction of gas flow, and the axes of the resonator and discharge are mutually perpendicular. In lasers of this structural design it proves possible to realize a pulse repetition rate up to several kilohertz.

This paper reports on the design of a compact periodic pulse CO_2 laser with gas circulation in a closed cycle, operating at frequencies up to 350 Hz with a degree of time stability of the radiation. A number of units similar in terms of output parameters have been described in the literature. However, data on the timewise stability of the radiation is either lacking in this literature [2, 3], or the average output power falls off rapidly with time [5].

A schematic of the laser setup is shown in Figure 1. Its working volume of 1.5 x 1.5 x 30 cm is formed by two flat stainless steel electrodes, the edges of which are rounded off to obtain a uniform discharge. Preliminary volumetric ionization of the gas mixture was accomplished by means of spark discharges, positioned at a distance of 10 cm from the resonator axis on the downstream side. Approximately 10% of the energy stored in the storage capacitor of 0.03 μF was split off to the discharges, where this capacitor was charged up to a voltage of ≈ 20 KV. Electrical power was supplied for the discharge by means of a TGI1-1000/25 thyratron. The laser resonator was formed by a fully enclosed metal reflector with a radius of curvature of 4 m and a germanium output reflector.

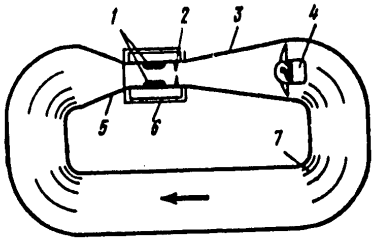

Figure 1. The configuration of the CO_2 laser.

Key: 1. Electrodes;
2. Pre-ionizer;
3. Diffuser;
4. Blower;
5. Nozzle;
6. Working chamber;
7. Turning blades (the direction of flow is shown with the arrow).

A gas mixture of CO_2:N_2:He = 1:1:8 at a pressure slightly above atmospheric pressure was used in the laser. The gas was pumped through the working volume in a closed cycle using an aerodynamic tube of stainless steel with a nozzle and a diffuser (the overall dimensions of 150 x 80 x 20 cm, a useful volume of ≈ 80 liters). The maximum flow velocity in the interelectrode gap was $\leq$ 10 m/sec and was varied by changing the rotational speed of the blower.

The energy in a single radiation pulse was 0.35 J. The pulse waveform was close to triangular with a steep leading edge (≈ 200 nsec) and a half-height of 3 μsec. The average radiation power is shown as a function of the pulse repetition rate in Figure 2. It can be seen that when $f \leq 150$ Hz, the function P(f) is linear. The deviation from a linear function at high frequencies is related to the insufficient pump-through velocity of the gas mixture; when $f > 350$ Hz, the discharge became unstable and the output power fell off sharply. We will note that at f = 350 Hz, the level of P reaches ≈ 70 watts.

For the case of CW operation at 100 Hz for 30 minutes without renewing the gas mixture, the average power fell off by no more than 15%. With further operation, arcs appeared in the discharge gap in individual pulses, which, however, had a weak influence on the size of P.

No special heat exchanger was provided in the laser and natural cooling of the gas mixture was used by virtue of the content with the surface of the pump-through tube and the turning blades. The gas temperature at the input to the discharge gap was monitored by means of a chromel-alumel thermocouple, the signal from which was fed to an autorecorder. It turned out that even with natural cooling, the gas mixture temperature during 30 minutes of laser operation at a frequency of 100 Hz did not rise above 50° C. Such an insignificant temperature increase should have no effect on the discharge stability.

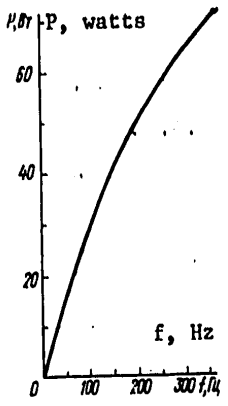

Figure 2. The output power as a function of the pulse repetition rate.

Contraction of the discharge and reduction of the output radiation power during long term operation of teh laser were, in our opinion, related to chemical reactions in the discharge plasma. Indicative of this, in particular, is the fact that with repeated, short term actuations of the laser, when the gas mixture temperature changed insignificantly (in a range of a few degrees), the discharge stability was determined by the total number of discharges, which was close to the corresponding number of discharges in the quasi-continuous mode. No chemical analysis was made in this work of the change in the composition of the gas mixture in the process of running the laser.

We will note in conclusion that in our experiments, the stability of the output radiation parameters increased even with a slight renewal (a few liters per minute) of the gas mixture.

BIBLIOGRAPHY

1. O.R. Wood, PROC. IEEE, 62, 355, (1974); TRUDY IIER, 62, No 3, 83 (1974).

2. A.E. Hill, APPL. PHYS. LETTS, 12, 324, (1968).

3. G.S. Dzakowic, S.A. Wutzke, J. APPL. PHYS., 44, 5061, (1973).

4. D.C. Hamilton, D.F. James, S.A. Ramsden, J. PHYS. E.: SCI. INSTR., 8, 849, (1975).

5. M.F. Turgeon, IEEE J., QE-7, 495, (1971).

8225
CSO:8144/1216

QUANTUM ELECTRONICS

UDC 535.375

SPATIAL POLARIZATION INVERSION OF A WAVE FRONT FOR THE CASE OF FOUR PHOTON INTERACTION

Moscow KVANTOVAYA ELEKTRONIKA in Russian Vol 6 No 3, 1979 pp 629-631

[Article by B.Ya. Zel'dovich and V.V. Shkunov, Physics Institute imeni P.N. Lebedev of the USSR Academy of Sciences, Moscow, manuscript received 2 Aug 78]

[Text] The problem of the wave front inversion of depolarized light is theoretically analyzed for the case of four-photon interaction. Methods which allow for total spatial polarization inversion are indicated.

The wave front inversion (OVF) of light in the case of stimulated back-scattering was studied in detail both experimentally [1] and theoretically [2]. Recently, following theoretical proposals of [3], OVF was experimentally realized on the basis of four-photon interaction (ChFV) [4]. All of these works applied to OVF of completely polarized beams. At the same time, in a number of OVF applications, it is necessary to invert a beam with a spatially inhomogeneous polarization state. The physical processes occuring with OVF of depolarized light using the stimulated scattering method have already been studied both theoretically and experimentally [5]. The problem of the OVF of depolarized radiation using the ChFV method is treated theoretically in this communication.

An abbreviated equation for an inverted wave $E_4(r)$ of frequency ω in a cubic medium is written in the form

$$\cos\theta \frac{\partial E_4}{\partial z} = i\frac{2\pi\omega^2}{c^2 k} \Pi P^{NL}; \quad (1)$$

$$(P^{NL})_i = (\chi_{iklm} + \chi_{ilkm}) E_{1k} E_{2l} E^*_{3m}, \quad (2)$$

where θ is the angle between the direction $n = k_4/k$ of the E_4 wave and the normal to the input surface of the nonlinear medium (the incident angle, read taking into account the refraction within the medium; see Figure 1); $k = \varepsilon^{1/2}\omega/c$. The operator $\Pi_{ik} = \delta_{ik} - n_i n_k$ of the projection onto a plane

perpendicular to the direction of E_4 beam propagation was likewise introduced in (1); the appearance of such an operator is related to the transverse nature of the electromagnetic waves. We assume that the wave E_3, which is to be inverted, and this also means the inverted wave E_4, occupy a comparatively small solid angle about the central direction n. Then the polarization vectors of these waves can be considered as falling the indicated plane. The quantity χ_{iklm} is the cubic nonlinearity tensor of the medium. Of all of the terms in the cubic polarization vectorP^{NL} we left only those which describe the excitation of the complex conjugate wave E_4 E_3^* in the presence of strong counter waves $E_1e^{ik_1r}$ and $E_2e^{-ik_1r}$ of the same frequency ω.

For practical applications, it is necessary to achieve total polarization inversion of the form $E_4(r)$ $E_3^*(r)$. At the same time, even within the nonlinear medium, as can be seen from (1) and (2), the polarization state of the E_4 wave differs in the general case from the requisite (E_3^*):

$$(E_4)_l \sim \Gamma_{lk} E^*_{3k};$$
$$\Gamma_{lk} = \Pi_{ls}(\chi_{sqlk} + \chi_{slqk}) e_{1q} e_{2l}, \qquad (3)$$

where e_1 and e_2 are complex unit vectors of the polarization of strong waves E_1 and E_2. In this case, we consider the unit vectors e_1 and e_2 to be constant over the entire volume of the nonlinear medium and we nelglect (in a Born approximation) the change in the E_3^* vector space. Moreover, the polarization state of both fields E_3 and E_4 can differ markedly in the case of oblique refraction at the boundary of a nonlinear medium.

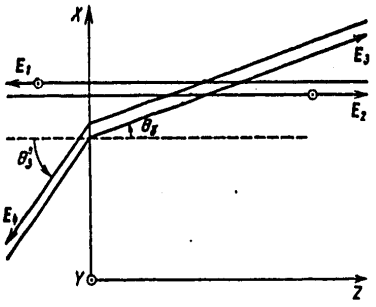

Figure 1.

If the fields of the incident and inverted waves in air are designated as B_3 and B_4, then in a Born approximation:

$$(B_4)_l = D_{lk}(B_3^*)_k; \quad D_{lk} = t'_{lm}\Gamma_{mi}t_{ik}. \qquad (4)$$

The two-dimensional matrix D_{ik} acts in a plane perpendicular to the direction n' of E_3 wave propagation in air. The matrix $\hat{t}$ describes the change in the electric field amplitude of the wave when entering the nonlinear medium, taking Fresnel reflection into account; the matrix $\hat{t}^*$ yields the same when exiting the medium.

We shall now pose the problem of achieving total spatial polarization OVF. For this, it is necessary to require that the two-dimensional matrix D_{ik} from (4) be a multiple of a unit matrix. For a medium with a specified tensor χ_{iklm}, we have available a number of free parameters, a variation of which can in principle achieve this result; thus, for example, one can vary the orientation and state of E_1 and E_2 strong wave polarization, employ transmitting

coatings, or change the orientation of the medium with respect to the direction of E_3 wave propagation.

We shall treat in more detail the case of an isotropic medium, for which

$$\chi_{ihlm} = \chi_1 \delta_{ih}\delta_{lm} + \chi_2 \delta_{il}\delta_{hm}. \quad (5)$$

The constants χ_1 and χ_2 can be determined from autofocusing tests and from the autorotation of the polarization ellipse (see for example, [6]). For a purely electronic nonlinearity mechanism, where $\omega << \omega_0$ (ω_0 are the main absorption bands), the relationship $\chi_1 = 2\chi_2$; this is apparently the situation for polycrystalline germanium at the wavelength of a CO_2 laser. For the Kerr nonlinearity (for example, the orientation of CS_2 molecules), $\chi_2 = 3\chi_1$; and for a strictional nonlinearity, $\chi_2 = 0$.

One of the possibilities of achieving total OVF (Figure 1) consists in the choosing of the incident angle θ_3' (in air). In this case, we are working from a configuration in which the plane-parallel layer of the nonlinear medium is placed inside the laser resonator. The polarization of both strong waves is chosen linear in the direction of the Y axis, perpendicular to the plane of drawing. The boundary of the nonlinear medium corresponds to the XY plane, while the beam being inverted E_3 falls in the XZ plane. Then the condition for precise inversion, $D_{ik} = \text{const} \cdot \delta_{ik}^{(2)}$, assumes the form

$$\chi_2/(\chi_1+\chi_2) = \cos^2(\theta_3 - \theta_3'). \quad (6)$$

Fresnel formulas for oblique incidence on to the nontransmitting surface were employed in deriving (6). We shall clarify the physical cause of precise reproduction, when condition (6) is met. The nonlinear polarization within the medium in our case is equal to

$$P^{HA} \equiv \hat{\Pi} P^{HA} = 2E_1E_2\{\chi_1 e_y(E_3 e_y) + \chi_2 E_3^*\}. \quad (7)$$

In the general case, $\chi_1 > 0$ and $\chi_2 > 0$, the E_3 wave component with Y polarization is inverted with a greater coefficient, greater by $(\chi_2 + \chi_1)/\chi_2$ times than the component orthogonal to it with polarization in the XZ plane. However, this latter component possesses a greater Fresnel transmission factor. Precise compensation of these two factors is achieved exactly when expression (6) is observed. For example, for germanium (an index of refraction of $n = 4$, $\chi_1 = 2\chi_2$), the angle $\theta_3' = 68.04°$ and $\theta_3 = 13.41°$. In this case, the single transit factor of the boundary (with respect to energy) for XZ polarization amounts to ≈ 0.96 (θ_3' is close to the Brewster angle); the same coefficient for Y polarization is equal to 0.32 (for the case of normal incidence, this quantity is identical for both polarizations and is equal to 0.64).

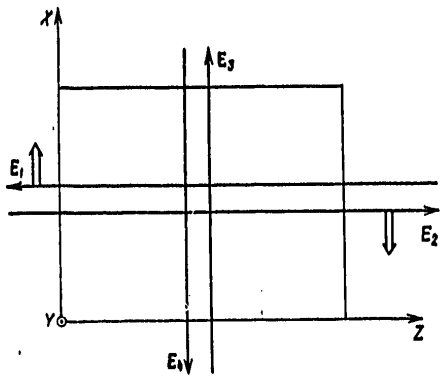

Figure 2.

Another configuration which realizes total OVF is shown in Figure 2. The E_1 and E_2 strong plane waves propagate along the Z axis and have a linear polarization e_X. The wave being inverted is introduced through the other boundary of the nonlinear medium (the YZ plane), where this wave propagates in the direction of the X axis. In this case:

$$\hat{\Pi}P^{\text{НЛ}} \equiv P^{\text{НЛ}} = 2\chi_3 E_1 E_1 E_3^* \qquad (8)$$

and refraction at the boundary likewise does not change the polarization state. We will note that transmission augmentation of all surfaces of the nonlinear medium can be employed in this configuration.

Finally, the latter configuration, which permits obtaining total OVF, corresponds to the case where all four waves propagate in a direction close to the normal to the boundary of the plane-parallel layer of the nonlinear medium. In this case, the projection operator can be replaced by a unit operator, and:

$$\hat{\Pi}P^{\text{НЛ}} = E_1 E_2 \{2\chi_3(e_1 e_2)E_3^* + \chi_4[(e_1 E_3^*)e_2 + (e_2 E_3^*)e_1]\}. \qquad (9)$$

It is not difficult to verify that $P^{\text{НЛ}}$ E_3' only in the single case where the the strong waves are circularly and mutually orthogonally polarized:
, or vice versa.

The authors are grateful to V.I. Kovalev and I.I. Sobel'man for their stimulating discussions.

BIBLIOGRAPHY

1. B.Ya. Zel'dovich, V.I. Popovichev, V.V. Ragul'skiy, F.S. Fayzullov, PIS'MA V ZHETF [LETTERS TO THE JOURNAL OF EXPERIMENTAL AND THEORETICAL PHYSICS], 15, 160 (1972);
V.V. Ragul'skiy, TRUDY FIAN [PROCEEDINGS OF THE PHYSICS INSTITUTE IMENI P.N. LEBEDEV OF THE USSR ACADEMY OF SCIENCES], 85, 8 (1976);
V. Wang, C.R. Giuliano, OPTICS LETTS, 2, 4 (1978);
B.Ya. Zel'dovich, N.F. Pilipetskiy, V.V. Ragul'skiy, V.V. Shkunov, KVANTOVAYA ELEKTRONIKA, 5, 1800 (1978).

2. V.G. Sidorovich, ZHTF [JOURNAL OF ENGINEERING PHYSICS], 46, 2168 (1976); I.M. Bel'dyugin, M.G. Galushkin, Ye.M. Zemskov, V.I. Mandrosov, KVANTOVAYA ELEKTRONIKA, 3, 2467, (1976); B.Ya. Zel'dovich, V.V. Shkunov, KVANTOVAYA ELEKTRONIKA, 4, 1090, 2353 (1977); 5, 36 (1978); N.B. Baranova, V.Ya. Zel'dovich, V.V. Shkunov, KVANTOVAYA ELEKTRONIKA, 5, 973 (1978).

3. R.W. Hellwarth, J. OPT. SOC. AMER., 67, 1 (1977); A. Yariv, D.M. Pepper, OPTICS LETTS, 1, 16 (1977); J. Marburger, APPL. PHYS. LETTS, 32, 372 (1978).

4. D. Bloom, G.C. Bjorklund, APPL. PHYS. LETTS, 31, 592 (1977); P.F. Liao, N.P. Economoy, R.R. Freeman, PHYS. REV. LETTS, 39, 1473 (1977). S.M. Jensen, R.W. Hellwarth, APPL. PHYS. LETTS, 32, 166 (1978); D.M. Bloom, P.F. Liao, N.P. Economoy, OPTICS LETTS, 2, 58, (1978). E.E. Bergman, I.J. Bigio, B.J. Feldman, R.A. Fisher, "Preprint LA-UR 78-1305 (1978); OPTICS LETTS (In press).

5. B.Ya. Zel'dovich, V.V. Shkunov, ZHETF, 75, 428 (1978); PREPRINT FIAN, Moscow, 1978, No 1. V.N. Blashchuk, B.Ya. Zel'dovich, V.N. Krashennikov, N.A. Mel'nikov, N.F. Pilipetskiy, V.V. Ragul'skiy, V.V. Shkunov, DAN SSSR [REPORTS OF THE USSR ACADEMY OF SCIENCES], 241, 1322 (1978); OPTICS COMMS, 27, 137 (1978). N.G. Basov, V.F. Yefimkov, I.G. Zubarev, A.V. Kotov, S.I. Mikhaylov, M.G. Smirnov, PIS'MA V ZHETF, 28, 215 (1978).

6. R.W. Hellwarth, PROGR. QUANT. ELECTRON., Vol 5, No 1 (1977).

8225
CSO:8144/1216

QUANTUM ELECTRONICS

UDC 535.375.5

THE INFLUENCE OF PUMP DEPLETION ON THE SUPERRADIATION PROCESS WITH RAMAN LIGHT SCATTERING

Moscow KVANTOVAYA ELEKTRONIKA in Russian Vol 6 No 3, 1979 pp 635-638

[Article by V.I. Yemel'yanov and V.N. Seminogov, Moscow State University imeni M.V. Lomonosov, manuscript received 7 Aug 78]

[Text] The process of superradiation for the case of Raman light scattering (SIKR) is analyzed in a single mode approximation taking pump depletion into account. The dynamics of population difference time waveform of the SIKR pulse are studied. It is shown that accounting for pump depletion clears up an additional condition of SIKR observation: an upper limit on the medium density at the $\approx 10^{19}$ cm^{-3}. It is noted that because of this, the observation of SIKR is more probable in gaseous media.

1. The superradiation effect for the case of Raman scattering (KR) of light (SIKR) in molecular and atomic systems is analyzed in an approximation of a specified pumping field in paper [1]. The scattered stokes radiation for the case of SIKR is produced in the form of a pulse, the width of which is $\tau_p \approx \approx 1/N$, where N is the number of scattering atoms. The scattered power in the case of SIKR is maximum at the point in time $t = t_m$ and is proportional to N^2. In the approximation of thespecified pumping field, the theoretical description of SIKR [1] proves to be similar to the description of the superradiation resonance process in a system of originally inverted two-level atoms [2, 3]. The conditions for observing SIKR are also similar: $t_m \approx \approx 1/n < T_2$ (T_2 is the transverse relaxation time, and n is the numerical density of the scattering particles). This means that for a specified pumping intensity, I_L, there exists a lower limit on the density of the medium, i.e., $n > n_{min}$ (I_L).

The SIKR process is treated in this paper taking pump depletion into account. An equation which describes population dynamics and the radiation power in the case of SIKR is derived and analyzed in a single mode approximation. It turns cut that accounting for pump depletion reveals an additional condition

for observing SIKR: besides the lower limit on n, there also exists an upper limit: $n_{min}(\tau_L) < n < n_{max} \approx 10^{19}$ cm^{-3}. This is related to the fact that the superradiative state arises at that point in time when the populations of the working levels of N particles are equalized by virtue of pump absorption. In a sufficiently dense medium, pump energy is depleted before this equalization occurs, and there is no superradiation. We will note that the value of n_{max} does not depend on the pumping intensity and is determined by the parameters of the medium. A numerical estimation of n_{max} shows that observing SIKR is most probable in gaseous media. Accounting for the motion of the population is the principle feature which distinguishes SIKR from the nonsteady-state KR mode, in the description of which one can neglect the change in the population [4].

Single mode effects of the SIKR process are not taken into account in this paper. Multimode SIKR theory has been developed in paper [5] in approximating a specified pump field.

2. We shall consider a system of N multilevel atoms (or molecules), enclosed in a volume V with a cylindrical shape (L and S are the length and cross-sectional are of the cylinder, the axis of the cylinder is directed along the X axis). The following electromagnetic field acts on the system:

$$E_L(x, t) = e_L\,(E_L^-(t)\,e^{-i(\omega_L t - k_L x)} + E_L^+(t)\,e^{i(\omega_L t - k_L x)}). \tag{1}$$

We shall assume that at the initial point in time p = 0, all of the atoms are in the ground state, while the average polarization is equal to 0. As a result, KR in the medium generates a stokes field at a frequency of $\omega_S = \omega_L - \omega_{ab}$, where $\omega_{ab} > 0$ is the transition frequency for the segregated pair of levels a and b (a is the upper level):

$$E_s(x, t) = e_s\,(E_s^-(t)\,e^{-i(\omega_s t - k_s x)} + E_s^+(t)\,e^{i(\omega_s t - k_s x)}. \tag{2}$$

We neglect the dependence of the slow amplitudes of $E^-_{L,S}(t)$ on x, assuming that the condition $\tau_p c > L$ is met.

We introduce the collective variables:

$$\rho_{ab} = \sum_\alpha \rho_{ab}^\alpha e^{-i(k_L - k_s)x_\alpha}; \quad D = \sum_\alpha D_\alpha = \sum_\alpha (\rho_{aa}^\alpha - \rho_{bb}^\alpha), \tag{3}$$

where ρ_{ab}^α is the slowly changing part of the nondiagonal element of the density matrix of an atom located at the point x_α; ρ_{aa}^α and ρ_{bb}^α are the populations of the a and b levels.

By employing the averaging method of [6], we obtain equations for ρ_{ab} and D:

$$\frac{\partial \rho_{ab}}{\partial t} + \frac{1}{T_2}\rho_{ab} = i\frac{r_{ab}}{\hbar} E_L^- E_s^+ D; \tag{4}$$

$$\frac{\partial D}{\partial t} = -\frac{2ir_{ab}}{\hbar}\left(E_L^- E_s^+ \rho_{ba} - E_L^+ E_s^- \rho_{ab}\right). \tag{5}$$

Here $$r_{ab} = \frac{1}{\hbar}\sum_p \left\{\frac{(d_{bp}e_L)(d_{pa}e_s)}{\omega_{bp}+\omega_L} + \frac{(d_{bp}e_s)(d_{pa}e_L)}{\omega_{bp}-\omega_s}\right\}.$$

The amplitude of the $E_L^-(t)$ field within the medium can be represented in the form of the sum of two parts:

$$E_L^-(t) = A + \mathcal{E}_L^-(t), \tag{6}$$

where A and $\mathcal{E}_L^-$ are the solutions of homogeneous and inhomogeneous Maxwell equations, and A corresponds to a pump field specified from without (A = = const).

The truncated Maxwell's equation for $\mathcal{E}_L^-$ has the form

$$\frac{\partial \mathcal{E}_L^-}{\partial t} + \gamma \mathcal{E}_L^- = -2\pi i\omega_L \frac{1}{V} r_{ba} E_s^- \rho_{ab}. \tag{7}$$

Here $\gamma = c/(2L)$ is a phenomenologically introduced field attenuation constant. Since an external field at a frequency of ω_s is lacking ($E_s^- = \mathcal{E}_s^-$), we write the equation for E_s^-:

$$\frac{\partial E_s^-}{\partial t} + \gamma E_s^- = -2\pi i\omega_s \frac{1}{V} r_{ab} E_L^- \rho_{ba}. \tag{8}$$

We shall assume that γ is the greatest of the inverse times of the problem, and the following conditions are met:

$$\gamma \gg 1/\tau_p,\ 1/t_m \gg 1/T_2. \tag{9}$$

When the right inequality of (9) is met, equations (4) and (5) have the integral of motions [1, 2]:

$$4\rho_{ab}\rho_{ba} + D^2 = R^2 = N^2 + 4N. \tag{10}$$

Neglecting the terms $d\mathcal{E}_L^-/\partial t$, $\partial \mathcal{E}_s^-/dt$, , we obtain the following from (7), (8) and (6):

$$E_L^- = \frac{A}{1+4\varkappa\rho_{ab}\rho_{ba}};\quad E_s^- = -\frac{2\pi i\omega_s}{\gamma V} r_{ab}\rho_{ba}\frac{A}{1+4\varkappa\rho_{ab}\rho_{ba}}, \tag{11}$$

where $\varkappa = \pi^2\omega_s\omega_L |r_{ab}|^2/\gamma^2 V^2$.

By substituting (11) in (4) and (5), and using (10), we derive the closed equation for D:

$$\frac{\partial D}{\partial t} = \Omega(R^2 - D^2)\frac{1}{[1+\varkappa(R^2-D^2)]^2};\quad D(0) = -N, \tag{12}$$

where $\Omega = 2\pi\omega_s |r_{ab}|^2 |A|^2/\hbar\gamma V$.

If the terms with κ (when $\kappa N^2 << 1$) are neglected in (12), then equation (12) becomes equivalent to equation (8) from paper [1], which describes SIKR in an approximation of a specifed pump field. The solution of (12) has the form:

$$\ln\{N|(R+D)/(R-D)|\} \approx 2\Omega t - 4\kappa N(D+N) - 2\kappa^2 N^2(D+N) + {}^2/_3\kappa^2 N(D^2+N^2). \quad (13)$$

In implicit form, the solution for D can also be represented in the form usually employed when describing the superradiative dynamics of the difference in population [1 - 3]:

$$D(t) = N\,\mathrm{th}\,[(t-t_m)/\tau_p]; \quad (14)$$

$$\tau_p = 1/(\Omega N); \quad (15)$$

$$t_m = {}^1/_2\tau_p\,[\ln N + 4\kappa N(D+N) + 2\kappa^2 N^2(D+N) - {}^2/_3\kappa^2 N(D^2+N^2)]. \quad (16)$$

we set $R \approx N$ with a precision of $1/N$ in (14) - (16).

By employing (11) and (12), the expression for SIKR power, $I_s(t) = 2\gamma V|\bar{E}_s|^2(2\pi)$, can be written in the form:

$$I_s(t) = \frac{\hbar\omega_s}{2}\Omega\frac{R^2-D^2}{[1+\kappa(R^2-D^2)]^2} = \frac{\hbar\omega_s}{2}\frac{\partial D}{\partial t}. \quad (17)$$

It follows from (14) and (17) that radiation is generated at the stokes frequency in the form of a pulse with a width τ_p, the maximum of which is achieved at the point in time t_m, in which case, at the point $t = p_m$, $D(t_m) = 0$ and the radiation power is $I_s(t_m) \approx N^2$.

If the terms with κ are neglected in formula (16), it transforms to the expression for the time delay derived in paper [1]. Thus, the condition for neglecting the pump depletion effect is the inequality:

$$\kappa N^2 < 1 \quad (18)$$

i.e., an upper limit is placed on the numerical density of the particles. When inequality (18) is violated, with an increase in the density n, t_m begins to grow proportionally to n^3. This quickly leads to a violation of the condition for observing SIKR: $t_m < T_2$. Thus, accounting for pump depletion specifies an additional condition for observing SIKR. From (18) and (11), we have:

$$n < \frac{c}{2\pi L\sqrt{\omega_s\omega_L}\,|r|} = n_{max}. \quad (19)$$

The result obtained can be explained with the following argument. The pumping field can be considered specified if the energy delivered over the radiation time τ_p is greater than the energy derived from the pumping field in the SIKR process:

$$[|A|^2/(2\pi)]\,c\tau_p S > n\hbar\omega_L SL.$$

Substituting τ_p from (15) in this expression, where Ω is specified in (12), we arrive at estimate (19).

When $L = 0.5$ cm, $\omega_s \approx \omega_L \approx 10^{15}$ s^{-1}, $|r| \approx 10^{-4}$ cgs ESU, we find $n_{max} \approx \approx 10^{19}$ cm^{-3}. Thus, observing SIKR is more probable in gaseous media.

The authors are grateful to S.A. Akhmanov and K.N. Drabovich for their useful discussions.

BIBLIOGRAPHY

1. S.G. Rautian, B.M. Chernobrod, ZHETF [JOURNAL OF EXPERIMENTAL AND ENGINEERING PHYSICS], 72, 1342, (1977).

2. R. Bonifacio, L.A. Lugiato, PHYS. REV. A, 11, 1507 (1975); 12, 587 (1975).

3. V.I. Yemel'yanov, Yu.L. Klimontovich, OPTIKA I SPEKTROSKOPIYA, 41, 913 (1976).

4. S.A. Akhmanov, K.N. Drabovich, A.G. Sukhorukov, A.S. Chirkin, ZHETF, 59, 485, (1970).

5. V.I. Yemel'yanov, V.N. Seminogov, "Tezisy II Vsesoyuz. konf. po spektroskopii kombinatsionnogo rasseyaniya" ["Topics of the Second All-Union Conference on Raman Scattering Spectroscopy"], Moscow, June, 1978.

6. V.S. Butylkin, Yu.G. Khronopulo, Ye.I. Yakubovich, ZHETF, 71, 1712 (1976).

8225
CSO:8144/1216

QUANTUM ELECTRONICS

UDC 535.375

ON THE POSSIBILITY OF FIELD WAVE FRONT INVERSION BY MEANS OF NONLINEAR OPTICS

Moscow KVANTOVAYA ELEKTRONIKA in Russian Vol 6 No 3, 1979 pp 638-641

[Article by I.M. Bel'dyugin, V.N. Seminogov and Ye.M. Zemskov, manuscript received 10 Aug 78]

[Text] It is shown that the effect of field wave front reversal can be manifest when fields interact at nonlinearities of any order. A classification is given for nonlinear processes which permit the observation of the indicated effect.

Nonlinear optical phenomena are well known at the present time, in which inversion of the wave fronts (OVF) of the interacting fields takes place: VRMB and VKR processes [1 - 3], the process of first and second harmonic mixing [4], as well as the four-wave parametric process of the form $2\omega_1 = \omega_2 + \omega_3$ [5]. It is shown in this paper that the field OVF effect is possible not only with the processes enumerated here, but also with the interaction of fields at nonlinearities of any order.

Let a field act on a system of two-level atoms (or molecules), where the field has several quasimonochromatic components at frequencies of ω_l:

$$E = \sum_l \mathcal{E}(\omega_l, r, z, t) \exp(i\omega_l t); \quad \omega_l = -\omega_{-l}; \quad \mathcal{E}(\omega_l, r, z, t) = \mathcal{E}^*(\omega_{-l}, r, z, t). \tag{1}$$

The frequencies of the existing fields satisfy several resonance conditions:

$$\sum_l n_l^{(s)} \omega_l = \omega_{21} + \nu_s, \tag{2}$$

where ω_{21} is the transition frequency for the segregated pair of levels; ν_3 is the mistuning from the s-th resonance; $n_l^{(s)} > 0$; $\sum_l n_l^{(s)} = q_s$ is the order of the s-th resonance.

With the action of field (1), nonlinear polarization appears in the medium, which we write in the form:

$$P(r, z, t) = \sum_l \mathcal{P}(\omega_l, r, z, t) \exp(i\omega_l t). \tag{3}$$

We shall assume that the field at a frequency ω_j propagates along the Z axis. Then the equation for the slowly changing amplitude of this field can be written in the form:

$$\frac{\partial e_j}{\partial z} + \frac{i}{2k_j}\Delta_\perp e_j = \frac{2\pi i\omega_j^2}{k_j c^2}\mathcal{P}(\omega_j, z, t)\exp(ik_j z), \tag{4}$$

where

$$\mathcal{E}(\omega_j, r, z, t) = e_j(r, z, t)\exp(-ik_j z); \quad k_j = -k_{-j}; \quad \Delta_\perp = \frac{\partial^2}{\partial x^2} + \frac{\partial^2}{\partial y^2}.$$

The amplitude of the nonlinear polarization arising in the medium is, in the general case, proportional to the product of the amplitudes of the interacting fields. If the process is described by nonlinear polarization of the type:

$$\mathcal{P}(\omega_j, r, z, t) \sim \mathcal{E}(\omega_j, r, z, t)\,|\mathcal{E}_{l_0}|^2 \prod_{l\neq j,\, l_0} [\mathcal{E}(\omega_l, r, z, t)]^{n_l} \tag{5}$$

(the fields at a frequency of ω_l with $l \neq j$, l_0 are plane ones, the amplitudes can be considered specified; the field at a frequency of ω_{l_0} propagates counter to the j-th wave), and the condition $l_m >> \lambda_{l_0}/\theta_{l_0}^2$ is met (l_m is the length of the medium, λ_{l_0} is the wavelength, θ_{l_0} is the diffraction divergence angle), then the propagation conditions for the j-th wave prove to be identical to the conditions treated in [1 - 3], and OVF of the j-th wave should occur.

However, if $l_m << \lambda_j/\theta_j^2$, while the process is described by polarization of the type

$$\mathcal{P}(\omega_j, r, z, t) \sim \mathcal{E}^*(\omega_j, r, z, t) \prod_{l\neq j} [\mathcal{E}(\omega_l, r, z, t)]^{n_l} \tag{6}$$

(the fields at a frequency of ω_l with $l \neq j$ are plane ones, and their amplitudes are specified), then the propagation conditions for the j-th wave are similar to the conditions treated in [4, 5], and OVF of the j-th wave should occur without a frequency shift.

Thus, the question of finding the processes in which OVF is possible reduces to finding the processes in which nonlinear polarization is described by expressions (5) or (6). General formulas for quasistatic polarization for any multiple photon process were derived in [6].

1. *Nonresonant Parametric Processes.* Let there be one resonance condition of the form:

$$\sum_l n_l\omega_l = 0; \quad \sum_l n_l = q. \tag{7}$$

The polarization amplitude at the frequency ω_j can be written as:

$$\mathcal{P}(\omega_j, r, z, t) = -\frac{T_2}{\hbar}\frac{i+(\nu-\Omega)T_2}{1+(\nu-\Omega)^2T_2^2}D_{0T}\left|\varkappa^{21}_{(q)}\right|^2\mathcal{E}(\omega_j)\left|\mathcal{E}(\omega_{l_0})\right|^2\prod_{l\neq j,\ l_0}\left|\mathcal{E}(\omega_l)\right|^{2n_l^{(1)}}. \tag{12}$$

The possible incoherent processes during which OVF can take place are shown in Figure 2.

3. *Resonant Parametric Processes.* are possible, where several resonance conditions (2) (s > 1) are met. For simplicity, we shall consider the case where there are two resonance conditions (s = 1, 2), where ω_1 enters into one resonance condition with a negative sign (s = 1), and does not enter into the second one at all (s = 2). An analysis of the general expression for the polarization [6] leads to the conclusion: in order to obtain polarization of the type (6), it is necessary that $n_j^{(1)} = 2$, and $n_l^{(2)}$ are arbitrary ($l \neq j$). The expression for the polarization is written in explicit form:

$$\mathcal{P}(-\omega_j, r, z, t) = -\frac{T_2}{\hbar}\frac{-i+(\nu-\Omega)T_2}{1+(\nu-\Omega)^2T_2^2}D_{0T}\times$$
$$\times\left\{2\left|\varkappa^{12}_{(q_1)}\right|^2\left|\mathcal{E}(\omega_j)\right|^2\mathcal{E}(-\omega_j)\prod_{l\neq j}\left|\mathcal{E}(\omega_l)\right|^{2n_l^{(1)}}+\right.$$
$$\left.+2\varkappa^{12}_{(q_1)}\varkappa^{21}_{(q_2)}\mathcal{E}^*(-\omega_j)\prod_{l\neq j}\left[\mathcal{E}(\omega_l)\right]^{n_l^{(1)}}\prod_{l}\left[\mathcal{E}^*(\omega_l)\right]^{n_l^{(2)}}\right. \tag{13}$$

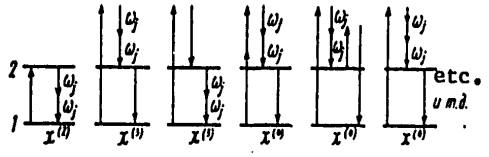

Figure 3.

Here, $\omega_1 < 0$; ω_l is included in expression (13) with the same sign as in the resonance condition (2).

If the first term in (13) can be neglected, then an expression is derived for polarization of the form of (6). This is easily achieved under experimental conditions, when $q_1 > q_2$. In contrast to the processes described in section 1, the processes considered here are resonance ones; they are shown in Figure 3.

The question of the phase matching of the interacting waves should be dealt with individually in each specific experimental situation.

BIBLIOGRAPHY

1. B.Ya. Zel'dovich, V.I. Popovichev, V.V. Ragul'skiy, F.S. Fayzulov, PIS'MA V ZHETF [LETTERS TO THE JOURNAL OF EXPERIMENTAL AND ENGINEERING PHYSICS], 15, 160, (1972).

$$\mathcal{P}(\omega_j, r, z, t) = n_j \varkappa^{*}_{(q)} [\mathcal{E}^{*}(\omega_j, r, z, t)]^{n_j - 1} \prod_{l \neq j} [\mathcal{E}^{*}(\omega_l, r, z, t)]^{n_l} \rho_{11}, \tag{8}$$

where $\varkappa_{(q)}$ is the polarizability of the q-th order; ρ_{11} is the population of the lower level; ω_j and ω_γ are chosen with the same sign with which they appear in resonance condition (7). It can be seen from (8) that to obtain polarization of the type (6), it is necessary that $n_j = 2$, n_γ is arbitrary ($\gamma \neq j$),

$$2\omega_j + \sum_{l \neq j} n_l \omega_l = 0, \text{ т. е.}$$

$$\mathcal{P}(\omega_j, r, z, t) = 2\varkappa^{*}_{(q)} \mathcal{E}^{*}(\omega_j, r, z, t) \prod_{l \neq j} [\mathcal{E}^{*}(\omega_l, r, z, t)]^{n_l} \rho_{11}. \tag{9}$$

The possible processes of this class are shown schematically in Figure 1.

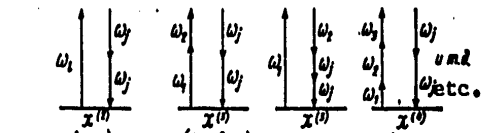

Figure 1.

2. *Incoherent Processes.* Let there be only one resonance condition of the form:

$$\sum_l n_l \omega_l = \omega_{21} + \nu; \quad \sum_l n_l = q. \tag{10}$$

The polarization amplitude at the frequency ω_1 is written as:

$$\mathcal{P}(\omega_j, r, z, t) = -\frac{T_2}{\hbar} \frac{i + (\nu - \Omega) T_2}{1 + (\nu - \Omega)^2 T_2^2} D_{cr} n_j |\varkappa^{21}_{(q)}|^2 \times$$

$$\times |\mathcal{E}(\omega_j)|^{2(n_j - 1)} \mathcal{E}(\omega_j) \prod_{l \neq j} |\mathcal{E}(\omega_l)|^{2n_l}, \tag{11}$$

where T_2 is the transverse relaxation time; Ω is the Stark level shift frequency; D_{ct} is the steady-state difference in the populations of the levels; ω_γ and ω_γ are incorporated in expression (11) with the same sign as in condition (10).

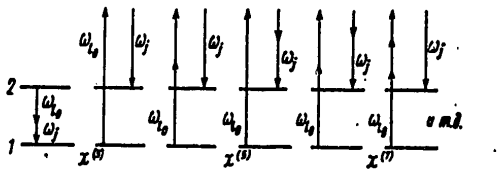

Figure 2.

It can be seen from (11) that to obtain polarization of the type (5), it is necessary that $n_j = 1$, $n_{\gamma_0} = 1$, n_γ is arbitrary ($\gamma \neq j, \gamma_0$), where $\omega_j + \omega_l + \sum_{l \neq j, l_0} n_l \omega_l = \omega_{21} + \nu$. . We then have:

2. I.M. Bel'dyugin, M.G. Galushkin, Ye.M. Zemskov, V.I. Mandrosov, KVANTOVAYA ELEKTRONIKA, 3, 2467, (1976).

3. V.G. Sidorovich, ZHTF [JOURNAL OF ENGINEERING PHYSICS], 46, 2168, (1976).

4. A. Yariv, OPTICS COMMS., 21, 49, (1977).

5. R.W. Hellwarth, J. OPT. SOC. AMER., 67, 1, (1977).

6. V.S. Butylkin, Yu.G. Khronopulo, Ye.I. Yakubovich, ZHETF, 71, 1712, (1976).

8225
CSO:8144/1216

QUANTUM ELECTRONICS

UDC 535.341

OPTICAL LOSSES IN KRS-5 AND KRS-6 CRYSTALS

Moscow KVANTOVAYA ELEKTRONIKA in Russian Vol 6 No 3, 1979 pp 646-648

[Article by V.G. Artyushenko, Ye.M. Bianov, L.V. Zhukova, F.N. Kozlov, V.I. Masychev, Ye.G. Morozov, and V.G. Plotnichenko, Physics Institute imeni P.N. Lebedev of the USSR Academy of Scineces, Moscow, manuscript received 1 Sep 78]

[Text] The bulk and surface absorption factors, as well as the total scattering factors in KRS-5 and KRS-6 crystals were measured laser calorimetry at wavelengths of 0.647, 1.06, 5.5 and 1.06 μm [sic]. The minimal volumetric absorption coefficients amount to $(3 - 5) \cdot 10^{-4}$ cm^{-1} (100 - 200 dB/km).

Materials which are transparent in the central IR band are attracting considerable attention for two basic reasons. In the first place, the radiation wavelengths of a number of high power lasers (CO_2, CO, DF and HF lasers) fall in this band. Secondly, the calculated fundamental absorption levels of many compounds in the central IR band are enormously lower than the limit of optical losses achieved in fused quartz in the 1.3 μm region and equal to 10^{-6} cm^{-1} (≈ 0.5 dB/km) [1].

In terms of the set of physical properties, one of the most promising materials, especially from the viewpoint of fiber optics, is the crystalls of solid solutions of thallium halides: KRS-5 (TlBr-TlJ) and KRS-6 (TlBr-TlCl). Thus, according to paper [2], the optical losses in them in the radiation range of a CO laser (≈ 5.5 μm) can achieve a level of 10^{-2} - 10^{-5} dB/km. At the present time, only the absorption factors of these crystals have been measured at a few wavelengths: in papers [3, 4], at 10.6 μm, and in paper [5], at 2.7 and 3.8 μm in KRS-5 crystals. The absorption factors in KRS-5 and KRS-6 crystals were not measured in the radiation range of a CO laser. Radiation scattering in the central IR band likewise has not been studied in these crystals, as far as we know.

The results of measurements of the bulk and surface absorption coefficients are given in this paper, as well as of the total scattering in KRS-5 and KRS-6 crystals at wavelengths of 0.647, 1.06, 5.5 and 10.6 μm.

The crystals which were investigated were grown by the Stockbarger method on seeds, oriented in the [100] crystallographic direction, and in this case, thallium halides were used as the initial material following repeated crystallization purification, carried out until the complete elimination of nontransparent material, even the upper part of the rods. Based on the data of spectral chemical analysis, cationic impurity content did not exceed the following values: for Ag, Mn $1 \cdot 10^{-6}$ % by weight, Cu $3 \cdot 10^{-6}$ % by weight, Cd, Pb, In $1 \cdot 10^{-5}$ % by wieght, Sn, Ni, Mg, Fe $3 \cdot 10^{-5}$ % by weight, and Al $5 \cdot 10^{-5}$ % by weight. Based on the data of a chemical analysis, the sulfur content in the samples was on the order of 10^{-5} % by weight. The oxygen content in the KRS-5 crystals, determined by activation analysis, did not exceed 10^{-5} % by weight. For the studies, the samples were cut in the form of cylindrical rods (50 mm x 5 mm diameter), oriented along the [100] crystal axis. For one part of the samples, the surfaces were polished, and for the other, they were subjected to chemical etching.

The bulk β_v and the surface $2\beta_s$ absorption factors were measured by means of laser calorimetry [6, 7] based on the initial slope of the heating curve. The influence of heat dissipation from the surface of the sample was taken into account using the procedure of [7]. The total scattering factor γ was measured in an Ulbricht sphere with a thermocouple radiation detector.

The bulk (β_v) and the surface ($2\beta_s$) absorption factor, and the total scattering factor (γ) in industrial samples of KRS-5 and KRS-6 at wavelengths of 0.647, 1.06, 5.5 and 10.6 μm (measurement precision: $\Delta\beta_v/\beta_v \leq 20\%$, $\Delta\beta_s/\beta_s \leq 3\%$, $\Delta\gamma/\gamma \leq 30\%$).

Образец Sample	λ, мкм micrometers								
	0,647		1,06		5,5			10,6	
	$10^4\beta_v$ ($см^{-1}$)	$10^4\gamma$ ($см^{-1}$)	$10^4\beta_v$ ($см^{-1}$)	$10^4\gamma$ ($см^{-1}$)	$10^4\beta_v$ ($см^{-1}$)	$10^4 2\beta_s$ ($см^{-1}$)	$10^4\gamma$ ($см^{-1}$)	$10^4\beta_v$ ($см^{-1}$)	$10^4\gamma$ ($см^{-1}$)
KPC-5[1]	14	210	3,6	50	3,3	3	21	5,1	2,4
KPC-5[1]	7,3	200	6,3	45	3,6	—	15	3,1	2,6
KPC-5[2]	41	170	18	51	11	—	19	13	4,6
KPC-6[1]	19	56	20	16	5,5	6	13	4,2	2,6
KPC-6[1]	28	58	10	13	3,5	10	14	6,0	2,9
KPC-6[2]	20	32	8,8	6	12	—	8	8,6	3,4
KPC-6[2]	9,7	14	3,4	9	10	—	12	7,0	1,2

1) Polished sample; 2) Etched sample.

The side surface of the samples was polished. To avoid the influence of surface scattering by the end faces, bulk scattering was measured in only

the central part of the sample (with a length of 1 cm), while the remaining side surface was enclosed with an absorbing jacket.

The following were used as the radiation sources: a "Spectra-Physics-164" krypton laser with a wavelength of $\lambda = 0.647$ μm, YAG:Nd^{3+} laser at $\lambda = 1.06$ μm, an industrial sealed-off CO laser with water cooling a radiation spectrum in the vicinity of $\lambda = 5.5$ μm, and a "LG-22" CO_2 laser at $\lambda = 10.6$ μm. It should be noted that since the CO laser employed had a rather wide radiation spectrum, the experimental results obtained yield average values in this spectral range.

The measurement results are presented in the table. The values of the absorption factor at the surface of both end faces are given only for a wavelength of 5.5 μm, since $\beta_v >> 2\beta_s$ was obtained for the remaining wavelengths. The scatter in the sizes of $2\beta_s$ for various samples indicates their dependence on the quality of surface treatment. A comparison of the surface absorption factors of the polished and etched surfaces allows for the hypothesis that the surface layer which is damaged and contaminated during polishing, and which is removed by etching, is a source of additional absorption of the through radiation. However, it must be noted that with chemical treatment of the surfaces, the etching of which is accomplished manually, there flatness is destroyed and they intensely scatter the through radiation.

It can be seen from the table that the levels obtained for the optical losses in the samples investigated considerably exceed the supposed fundamental loss level; in this case, the minimum bulk absorption factors amount to $(3-5) \cdot 10^{-4}$ cm^{-1}, which corresponds to 120-200 dB/km. The exceptionally high total scattering factors in these crystals should also be noted, which significantly exceed the bulk absorption factors for all wavelengths, with the exception of $\lambda = 10.6$ μm. Preliminary estimates show that most likely, the basic cause of such a high scattering level is scattering at the end faces of the samples.

In conclusion, the authors express their gratitude to T.I. Darvoid, V.B. Neustruyev and Ye.P. Nikitin for their assistance in performing the work and their useful discussions.

BIBLIOGRAPHY

1. M. Horiguchi, T. Osanai, ELECTR. LETTS., 12, 310 (1976).

2. D.A. Pinnow, A.L. Gentlee, A.G. Standlee, A.I. Timper, L.M. Hobrock, APPL. PHYS. LETTS., 33, 1, 28 (1978).

3. T.I. Darvoid, Ye.K. Karlova, N.V. Karlov, G.P. Kuz'min, I.S. Lisitskiy, Ye.V. Sisakyan, KVANTOVAYA ELEKTRONIKA, 2, 765 (1975).

4. V.G. Dorofeyev, V.A. Kareva, V.S. Makin, V.N. Smirnov, OPTIKO-MEKHANICHESKAYA PROMYSHLENNOST' [THE OPTOMECHANICAL INDUSTRY], 6, 35, 1978.

5. I.A. Harrington, Proc. 8th ASTM Symp. on Laser Ind. Damage in Opt. Mater., 2, 45, (1976).

6. V.G. Artyushenko, Ye.M. Dianov, Ye.P. Nikitin, KVANTOVAYA ELEKTRONIKA, 5, 1065, (1978).

7. H.B. Rosenstock, M. Hass, D.A. Gregory, I.A. Harrington, APPL. OPTICS, 16, 2837, (1977).

8225
CSO:8144/1216

END